The FEBS Journal

FEBS PRESS science publishing by scientists

Oncogene c-fos and mutant R175H p53 regulate expression of Nucleophosmin implicating cancer manifestation

Parijat Senapati[1,†], Suchismita Dey[1], Deepthi Sudarshan[1,‡], Sadhan Das[1,†], Manoj Kumar[1,§], Stephanie Kaypee[1], Azeem Mohiyuddin[2], Gopinath S. Kodaganur[2,3] and Tapas K. Kundu[1]

1 Transcription and Disease Laboratory, Molecular Biology and Genetics Unit, Jawaharlal Nehru Centre for Advanced Scientific Research (JNCASR), Bangalore, India
2 Sri Devaraj Urs Academy of Higher Education and Research (SDUAHER), Kolar, India
3 Bangalore Institute of Oncology (BIO), Bangalore, India

Keywords
AP-1 transcription factor; cancer; gene regulation; mutant p53; promoter

Correspondence
T. K. Kundu, Molecular Biology and Genetics Unit, JNCASR, Jakkur, Bangalore-560064, Karnataka, India
Fax: +91 80 22082766
Tel: +91 80 22082840
E-mail: tapas@jncasr.ac.in

Present addresses
[†]Department of Diabetes Complications and Metabolism, Diabetes Metabolism Research Institute, Beckman Research Institute of City of Hope, Duarte, CA 91010, USA
[‡]St-Patrick Research Group in Basic Oncology, Laval University Cancer Research Center, CHU de Québec Research Center-Oncology Axis, Quebec City, QC, G1R 3S3, Canada
[§]School of Biological and Environmental Sciences, Faculty of Basic Sciences, Shoolini University, Solan, Himachal Pradesh, India

Parijat Senapati and Suchismita Dey contributed equally to this work

(Received 1 December 2017, revised 15 June 2018, accepted 3 August 2018)

doi:10.1111/febs.14625

Nucleophosmin (NPM1) is a nucleolar protein that is frequently overexpressed in various types of solid tumors. NPM1 is involved in several cellular processes that might contribute significantly to the increased proliferation potential of cancers. Previous reports suggest that NPM1 expression is highly increased in response to mitogenic and oncogenic signals, the mechanisms of which have not been elucidated extensively. Using constructs incorporating different fragments of the NPM1 promoter upstream to a Luciferase reporter gene, we have identified the minimal promoter of NPM1 and candidate transcription factors regulating NPM1 promoter activity by luciferase reporter assays. We have validated the roles of a few candidate factors at the transcriptional and protein level by quantitative reverse transcriptase PCR, immunoblotting and immunohistochemistry, and explored the mechanism of regulation of NPM1 expression using immunoprecipitation and chromatin immunoprecipitation assays. We show here that the expression of NPM1 is regulated by transcription factor c-fos, a protein that is strongly activated by growth factor signals. In addition, mutant p53 (R175H) overexpression also enhances NPM1 expression possibly through c-myc and c-fos. Moreover, both c-fos and mutant p53 are overexpressed in oral tumor tissues that showed NPM1 overexpression. Collectively, our results suggest that c-fos and mutant p53 R175H positively regulate NPM1 expression, possibly in synergism, that might lead to oncogenic manifestation.

Abbreviations
ANOVA, one-way analysis of variance; AP-1, activator protein 1; AP1BS, AP-1-binding site; CBP, cAMP response element-binding (CREB) binding protein; CCNA2, cyclin A2; CCNB2, cyclin B2; CDC25C, cell division cycle 25C; CDK1, cyclin-dependent kinase 1; CDKN1A, cyclin-dependent kinase inhibitor 1A; c-fos, Fos proto-oncogene, AP-1 transcription factor subunit; ChIP, chromatin immunoprecipitation; c-jun, Jun proto-oncogene, AP-1 transcription factor subunit; CMV, cytomegalovirus; c-myc, MYC proto-oncogene, basic helix loop helix (bHLH) transcription factor; CP, core promoter; Dox, doxycycline; FBS, fetal bovine serum; FLAG, FLAG octapeptide tag; HCV, hepatitis C virus; HDAC, histone deacetylase; HEK293, human embryonic kidney cells 293; IgG, immunoglobulin G; MDM2, Mouse Double Minute 2; mRNA, messenger ribonucleic acid; mut, mutant; mutp53, mutant p53; NF-Y, nuclear transcription factor Y; NPM1, nucleophosmin; Nut-3a, Nutlin 3a; OSCC, oral squamous cell carcinoma; p300, E1A-binding protein p300; p53, tumor protein p53; PBS, phosphate buffered saline; Ras, RAS proto-oncogene, GTPase; RT, room temperature; RT-qPCR, reverse transcriptase – quantitative polymerase chain reaction; SEM, standard error of mean; si-RNA, silencing RNA; si-scr, scrambled (negative control) si-RNA; STAT3, signal transducer and activator of transcription 3; TATA, TATA box promoter element; TFIIB, transcription factor II B; TSS, transcription start site; WT, wild-type; YY1, Ying Yang 1.

Introduction

Nucleophosmin (NPM1) is a multifunctional protein that is predominantly nucleolar and described to have oncogenic as well as tumor suppressor properties. Deletion or mutation of NPM1 is commonly found in hematological malignancies such as acute myeloid leukemia, acute promyelocytic leukemia, anaplastic large cell lymphoma, and in premalignant myelodysplastic syndrome [1]. On the contrary, NPM1 is overexpressed in human tumors of diverse histological origins such as gastric [2], colon [3], breast [4], ovary [5], bladder [6], oral [7], thyroid [8], brain [9], liver [10], prostate [11,12] and multiple myeloma [13]. NPM1 overexpression correlates well with the clinical features of cancer in some of the cases. For example, overexpression of NPM1 in hepatocellular carcinoma correlates well with clinical prognostic parameters such as serum alpha fetal protein levels, tumor pathological grading and liver cirrhosis [10], suggesting that NPM1 overexpression could serve as a diagnostic marker for hepatocellular carcinoma. NPM1 overexpression and hyperacetylation progress according to the increasing grade of the tumor in oral squamous cell carcinoma (OSCC) [7]. Moreover, NPM1 overexpression also correlates well with recurrence and progression of bladder cancer to advanced stages [6] and is associated with acquired estrogen-independence in human breast cancer cells [4]. In gastric cancer, NPM1 expression is correlated with resistance to the drug oxaliplatin [14].

Notably, NPM1 is a direct transcriptional target of oncogenic transcription factor c-myc [15] and NPM1 overexpression alone can promote the transformation of NIH3T3 mouse fibroblast cells [16]. NPM1 suppresses apoptosis and promotes DNA repair thereby aiding in the survival of tumor cells where NPM1 is overexpressed [1,17]. In addition, NPM1 overexpression promotes cell division and growth, presumably through stimulatory effects on ribosomal DNA (rDNA) transcription, ribosome subunit export and DNA replication during S phase [1]. NPM1 overexpression also interferes with ARF (Alternate reading frame product of the CDKN2A locus)-mediated activation of p53 thereby further contributing to oncogenesis. Similar to oncogenes such as Ras, overexpression of NPM1 also causes cellular senescence in human fibroblast cells [18]. Moreover, NPM1 is induced upon mitogenic signals in T cells, B cells and the mouse fibroblast Swiss 3T3 cells [19–21]. All these studies suggest that NPM1 overexpression promotes tumor development and hence could function as a proto-oncogene. NPM1 is also known to respond to various cellular stresses. NPM1 mRNA, as well as protein levels, are rapidly induced in response to ultraviolet radiation or thymine dinucleotide treatment that mimics a DNA damage signal [22]. It is also induced in hypoxic conditions in normal and cancerous cells through HIF-1α (Hypoxia inducible factor 1 alpha subunit) binding to its promoter and prevents apoptosis of cells in these conditions [23]. These studies show that NPM1 expression is regulated by oncogenic signals and cellular stresses and hence it is of vital importance to study the regulation of NPM1 gene expression.

Till date, there are only a few reports that have tried to address the regulation of NPM1 expression at the level of transcription. The first study on NPM1 gene regulation showed that the NPM1 promoter has a Yin Yang 1 (YY1) binding site at −371 to −344 nucleotide position upstream to the transcription start site (TSS) [24]. Subsequently, it was shown that the YY1 response element on NPM1 promoter is bound by YY1-HDAC (histone deacetylase) repressor complex. Upon infection by Hepatitis C virus (HCV), the YY1-HDAC repressor complex is replaced by the YY1-p300-NPM1-HCV core transcription activation complex, relieving its repression and inducing NPM1 expression during HCV infection [25]. NPM1 has also been identified as a myc responsive gene by a subtractive hybridization screen [15]. Ras signaling leads to c-myc recruitment to the NPM1 promoter in U1 bladder cancer cells [26]. Conversely, differentiation of human leukemic HL-60 cells into mature granulocytic cells by retinoic acid (RA) leads to reduction in total c-myc levels as well as on NPM1 promoter and consequently to a reduction in NPM1 levels [27]. Further, Interferon alpha (IFN-α) stimulation of Jurkat cells (immortalized T lymphocyte cells) causes increased phosphorylation of Signal transducer and activator of transcription 3 (STAT3) that enhances its nuclear localization and binding to the NPM1 promoter, leading to a concomitant rise in NPM1 expression levels. Interestingly, NPM1 binds to phospho-STAT3 and is responsible for its nuclear translocation [28]. A recent report suggests that mTOR (mechanistic target of rapamycin) kinase transcriptionally regulates NPM1 expression by directly binding to the NPM1 promoter [29]. Although these studies shed some light into the regulation of NPM1 expression, a systematic study investigating the involvement of other oncogenic transcription factors apart from c-myc has been lacking.

Here, we show that NPM1 gene is regulated by an important oncogenic transcription factor c-fos/AP-1 and a prevalent gain-of-function mutant of tumor

suppressor p53, R175H, whereas wild-type (WT) p53 has no appreciable effect on NPM1 expression. Moreover, c-fos and mutant p53 levels are significantly upregulated in tumor tissues where NPM1 overexpression is observed confirming the role of a mutp53-c-fos axis in upregulating NPM1 expression in the context of cancer.

Results

Characterization of human NPM1 promoter

To understand the regulation of NPM1 expression, we set out to systematically characterize the regulatory elements of the human NPM1 gene. NPM1 gene is present on the long arm (5q35.1) of chromosome 5. The sequence co-ordinates for NPM1 gene locus according to NCBI accession no. NC_000005.9 are 170814708 to 170837888 in the hg19 assembly of the human genome. The TSS as reported in NCBI database is located at position 170814708, however, it differs from the experimentally identified TSS [24].The translation start codon ATG is present 246 bp downstream to the database TSS and is contained within exon 1. We consider the database TSS as +1 or TSS for all future references. In order to identify the minimal promoter for NPM1 gene, several fragments containing sequences upstream and downstream of the TSS were cloned into the pGL3 basic vector (Fig. 1A). Luciferase reporter assays were performed after transfection of different NPM1 promoter constructs (refer Fig. 1A) in HEK293 (human embryonic kidney 293) cells. Among all the promoter constructs, NPM1 Luc 2, 3 and 5 showed the highest relative luciferase activity (Fig. 1A). Interestingly, the data indicated that the upstream sequences (about 1–2 kb upstream relative to TSS) have maximal promoter activity and may contain activating transcription factor-binding sites. On the other hand, relatively lower luciferase activities (~50–100 fold lower) were observed with constructs containing regions downstream of the TSS especially Intron 1 (NPM1 Luc1 and NPM1 Luc4) (Fig. 1A). Upon analyzing the sequence upstream and downstream of the NPM1 TSS, we identified the core promoter elements, namely BREu (upstream transcription factor II B (TFIIB) recognition element), BREd (downstream TFIIB recognition element), TATA and INR (Initiator motif) [30], to be present downstream to the TSS (Fig. 1B). To further validate the importance of the core promoter elements, we constructed deletion constructs of the NPM1 promoter lacking these promoter elements (Fig. 1C). Luciferase assays performed using these constructs showed that the deletion of the core promoter elements led to a nearly 100-fold decrease in the promoter activity compared to respective full-length constructs (Fig. 1C). This result shows that indeed the sequence downstream to the TSS (+1 to +264) contains the core promoter elements and is required for NPM1 promoter activity. However, the upstream sequences may be a part of the upstream regulatory region of NPM1 and contain binding sites for several transcription factors that help in increased transcription of NPM1 gene. We used the upstream 1 kb sequence to predict the transcription factor-binding sites, using TRANSFAC and Consite databases [31]. The predicted transcription factor-binding sites are shown in Tables 1 and 2, respectively. Interestingly, we found binding sites for numerous transcription factors such as SNAI1, c-fos among others and previously reported factors such as c-myc. Of particular interest to us was c-fos which has been previously implicated in regulating genes involved in cell proliferation. The c-fos protein heterodimerizes with members of the JUN family of proteins such as c-jun, to form the transcriptional activator AP-1 (Activator Protein-1) [32–34]. The transcription factors, c-fos and c-jun, are categorized as immediate early genes and are the first responders to extracellular signals including growth factors, mitogens, and stress. They provide immediate but short acting signals, leading to varied cellular responses, some of which include differentiation, metabolism, and proliferation [35].

c-fos is highly expressed in many cancers including breast cancer [36], endometrial cancer [37], pancreatic cancer [38], and hepatocellular carcinoma [39]. The oncogenic mechanism of AP-1 includes regulation of genes involved in invasion, metastasis, angiogenesis, hypoxia to name a few. [40,41]. The fact that NPM1 expression is induced upon addition of serum, a source of growth factors, [20] suggests NPM1 could be induced downstream of AP-1. Moreover, c-fos and c-jun were also shown to be overexpressed in oral cancers [42,43]. Interestingly, c-fos expression is considered as a prognostic marker for cancer progression in some cancers, which correlates with our previous study demonstrating NPM1 overexpression and hyperacetylation in increasing grades of oral cancer [7]. These data encouraged us to investigate the role of AP-1 in the overexpression of NPM1 in cancer.

Transcription factor c-fos regulates NPM1 expression

To test whether transcription factor c-fos is involved in regulating NPM1 expression, the coding sequence of c-fos gene was cloned into the pFLAG-CMV2 vector. The ability of c-fos to activate NPM1 promoter activity was tested in HEK293 cells by co-transfecting it with NPM1

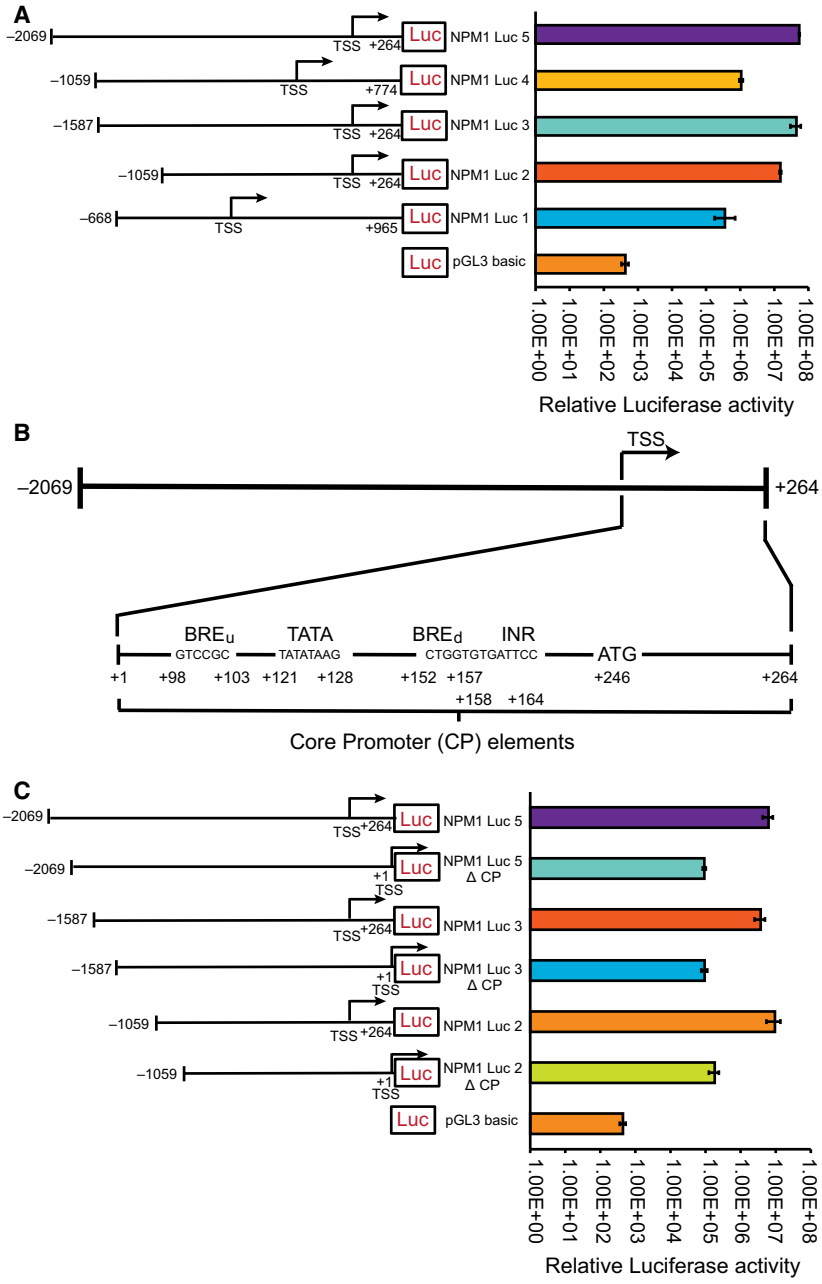

Fig. 1. Identification of NPM1 core promoter elements. (A) and (C) Bars represent relative Luciferase activity of the different NPM1 promoter constructs as indicated post 24 h of transfection (50 ng) in HEK293 cells. Data were normalized to internal transfection control β-galactosidase. Values are mean ± SEM from two independent experiments. Schematic representation of the constructs used is shown on the left. CP: core promoter. (B) Schematic representation of the putative NPM1 promoter region tested, with core promoter elements highlighted.

promoter construct NPM1 Luc 5 (−2069 to +264). A dose-dependent increase in NPM1 promoter activity was observed upon c-fos transfection, and 400 ng of c-fos resulted in approximately 8-fold increase in its activity (Fig. 2A). To confirm that c-fos enhances NPM1 promoter activity by binding to the upstream regulatory elements, the luciferase assays were performed with the core promoter deleted construct NPM1 Luc 5 ΔCP (−2069 to +1) (Fig. 2B). Significantly, the core-promoter deleted construct showed a similar dose-dependent increase in promoter activity after c-fos transfection (Fig. 2B). Deletion of the core-promoter elements did not affect the c-fos induced increase in promoter activity as evident from the similar fold change in luciferase activity (Fig. 2A versus Fig. 2B). Furthermore, to confirm that the promoter activation by c-fos is truly relevant to the cellular context, we performed luciferase assays in parallel with YY1, a transcription factor previously reported to activate NPM1 expression. [24] (Fig. 2C). These results show that c-fos enhances NPM1 promoter activity possibly by binding to the upstream regulatory elements of NPM1 promoter.

Table 1. List of transcription factor-binding sites predicted using TRANSFAC database. Only one high scoring site for each transcription factor is shown.

Matrix	Factor name	Position (strand)	Core score	Matrix score	Sequence
V$AP1_Q6_02	AP-1	499 (+)	0.936	0.942	TGATTcag
V$ARID5A_03	Arid5a	354 (+)	1	0.96	caAATATtcgaatt
V$CREBP1_01	ATF-2 group	526 (+)	1	1	TTACGtaa
V$BCL6_Q3_01	BCL-6 factors	619 (+)	0.984	0.937	cTTCCTaaca
V$BEN_01	BEN	978 (+)	1	0.983	CAGCGgag
V$BLIMP1_Q4	Blimp-1	1205 (−)	1	0.957	CTTTCcctggtg
V$BRCA_01	BRCA1	231 (+)	1	0.978	ataTGTTG
V$CEBPA_Q6	C/EBP group	523 (+)	0.975	0.97	aagttaCGTAAag
V$CP2_Q6	CP2-related factors	650 (+)	1	0.981	ctcTCTGGca
V$E2F_Q6_01	E2F-related factors	875 (−)	1	0.928	tctTGGCGggag
V$EGR1_Q6	EGR1 group	1047 (+)	1	0.953	gtGGGGGcga
V$ETS_Q6	Ets-related factors	560 (−)	1	0.987	caGGAAGg
V$HNF3B_Q6	FOX factors	224 (+)	1	0.967	tTGTTTgat
V$GEN_INI_B	general initiator	209 (+)	0.99	0.99	cctCACTT
V$GLI_Q3	GLI group	450 (−)	1	0.945	gcCCACCctc
V$GMEB2_04	GMEB	526 (−)	1	1	tTACGTaa
V$HES1_Q6	HES-1 group	1126 (+)	1	0.958	agCACGCgcg
V$HIF1A_Q5	HIF1	909 (+)	1	0.991	ggACGTGga
V$RUSH1A_02	hltf	534 (−)	1	0.998	agATAAGgac
V$HMGIY_Q3	HMGA factors	708 (−)	1	0.949	gtaaaAAATTcctga
V$HNF4A_Q3	HNF-4 group	661 (−)	1	0.931	ctgaaCTTTGgggt
V$HNF1A_Q4	HNF1-like factors	671 (+)	1	0.965	gggtaacgATTAActg
V$HSF1_01	HSF dimer	1307 (+)	0.974	0.977	GGAAGattcg
V$EKLF_Q5_01	KLF1 group	985 (−)	1	0.99	gGGGTGgggc
V$LRH1_Q5_01	LRH-1 group	478 (−)	1	0.976	tgtCCTTGcta
V$MAF_Q4	MAF group	498 (−)	0.93	0.912	cTGATTcagt
V$MAZ_Q6_01	MAZ	979 (+)	1	0.966	agcGGAGGgtggg
V$MAZR_01	MAZ group	984 (+)	0.93	0.952	aggggTGGGGcca
V$MUSCLEINI_B	muscle initiator	282 (−)	1	0.947	gcccgcgGGGTGctggggtgc
V$MYB_Q4	Myb-like factors	17 (+)	1	0.985	ggaaCAGTTaaa
V$NF1_Q6	NF-1 factors	875 (+)	1	0.984	tcTTGGCgggaggccggc
V$NKX25_Q6	Nkx group	718 (−)	1	0.969	cctgAAGTGat
V$P53_Q3	p53-related factors	741 (−)	0.993	0.964	gagGCTTGcag
V$REST_Q5	REST	286 (+)	1	0.916	gcggggTGCTGgg
V$SF1_Q5_01	SF-1 group	478 (+)	1	0.971	tgtCCTTGc
V$SOX2_Q3_01	Sox-related factors	575 (+)	1	0.99	tgaaaaACAAAgttc
V$SOX10_Q3	Sox10	626 (+)	0.992	0.985	ACAAAgaa
V$SP1_Q6_01	Sp1 group	985 (+)	0.945	0.959	ggGGTGGggc
V$SREBP_Q6	SREBP factors	1209 (−)	0.992	0.985	ccctggTGTGAttcc
V$STAT1_Q6	STAT factors	145 (−)	0.991	0.98	tTTCCTgtaa
V$TATA_01	TBP-related factors	1179 (+)	0.936	0.939	atATATAagcgcggg
V$TBX5_01	TBX5	315 (+)	1	0.963	caaGGTGTagct
V$TEF1_Q6_04	Tef-1-related factors	407 (−)	1	0.996	aggaGGAATgt
V$XVENT1_01	Xvent-1	351 (−)	1	0.902	tccCAAATattcg
V$DELTAEF1_01	ZEB1 group	655 (+)	1	0.987	tggCACCTgaa
V$ZFP206_01	Zfp206	1081 (−)	1	0.988	gcgctTGCGCa

Transcription factor AP-1 regulates NPM1 expression by directly binding to its promoter

In addition to HEK293 cells, we validated the luciferase reporter assay results in the human non-small cell lung carcinoma cell line, H1299 (Fig. 2D). c-fos enhanced the NPM1 promoter NPM1 Luc 2 (−1059/+264) activity in a dose-dependent manner as observed in HEK293 cells. Since c-fos binds to AP-1-binding sites on DNA as a heterodimer with c-jun [32], we checked the promoter activity of NPM1 upon co-transfection of c-fos and c-jun. Results showed that co-transfection of c-fos and c-jun led to a significant

Table 2. List of transcription factor-binding sites predicted using Consite database. Only one high scoring site for each transcription factor is shown.

Transcription factor	Sequence	From	To	Score	Strand
AGL3	CTATATATAA	1177	1186	8.008	–
AML-1	AGCCGCAAT	636	644	8.12	–
ARNT	CACGCG	956	961	7.103	–
Athb-1	CTATCATT	195	202	8.654	+
Broad-complex_1	AATTTGTTTGATAT	221	234	9.396	–
Broad-complex_4	AAGTAAAAAAT	706	716	9.84	+
bZIP911	GAGGACGTGGAA	907	918	10.5	+
c-FOS	CTGATTCA	498	505	8.378	+
c-REL	GGAAAGCACG	950	959	9.177	–
CF2-II	CTATATATAA	1177	1186	11.6	+
CFI-USP	GGGGTAACGA	670	679	9.784	+
COUP-TF	TGAACTTTGGGGTA	662	675	9.029	+
CREB	CAAGTCACCCGC	387	398	8.421	–
Dorsal_1	GGGGTGTCTTCC	174	185	8.362	+
Dorsal_2	GGTGTCTTCC	176	185	8.658	+
E2F	TTTGGCCC	513	520	8.832	+
E4BP4	AAGTTACGTAA	523	533	13.66	–
E74A	CAGGAAG	560	566	9.644	+
FREAC-4	GTAAAAAA	708	715	9.167	+
Hen-1	CAGCAGCGGAGG	975	986	8.185	–
HFH-1	AACTGTTCATT	99	109	8.706	+
HFH-2	AAAAAAAGATTA	248	259	9.784	–
HFH-3	TTAAATTTGTTT	218	229	9.008	+
HLF	AGTTACGTAAAG	524	535	9.539	+
HMG-IY	GTGTCTTCCTTTCTGA	177	192	8.019	–
HNF-1	GGTAACGATTAACT	672	685	13.36	–
HNF-3beta	AAGTAAAAAATT	706	717	10.36	–
Max	GAGGACGTGG	907	916	6.75	+
MEF2	CTATATATAA	1177	1186	12.3	–
Myc-Max	GAGGACGTGGA	907	917	9.902	+
Myf	CGACAGCAGCGG	972	983	10.48	+
n-MYC	CACGCG	956	961	7.79	+
NF-kappaB	GTTAATTCCC	333	342	9.145	–
NRF-2	GTCTTCCTTT	179	188	9.24	–
p65	GGAAAGCACG	950	959	7.822	–
Pbx	TTTGTTTGATAT	223	234	11.02	–
Snail	CACCTG	658	663	10.74	–
Sox-5	AAATAAT	156	162	7.499	+
SOX17	GACACTGAA	122	130	7.165	–
Spz1	AGGGTTGGAGG	918	928	9.182	+
SQUA	CTTCTTAAATTTGT	214	227	7.345	–
Staf	GCAGGGCACTAGGGGATGGG	748	767	11.64	–
TBP	ATATATAAGCGCGGG	1179	1193	13.06	+
TEF-1	AGGAGGAATGTT	407	418	12.54	–
Thing1-E47	CGACTGGAAA	945	954	7.556	+
USF	GACGTGG	910	916	6.973	+

increase in the promoter activity of NPM1 as compared to c-fos or c-jun alone. (Fig. 2E). This shows that AP-1 (c-fos/c-jun heterodimer) enhances NPM1 promoter activity. We next checked whether c-fos directly binds to NPM1 promoter. We used Consite database to predict the c-fos-binding sites on NPM1 promoter. At 80% cut-off, four putative-binding sites of c-fos were predicted based on the consensus-binding motif. We refer to them as AP-1-binding sites (AP1BS) based on score (Fig. 2F and Table 3). To demonstrate that c-fos binds to the AP-1-binding sites on NPM1 promoter, the four c-fos binding sites were mutated

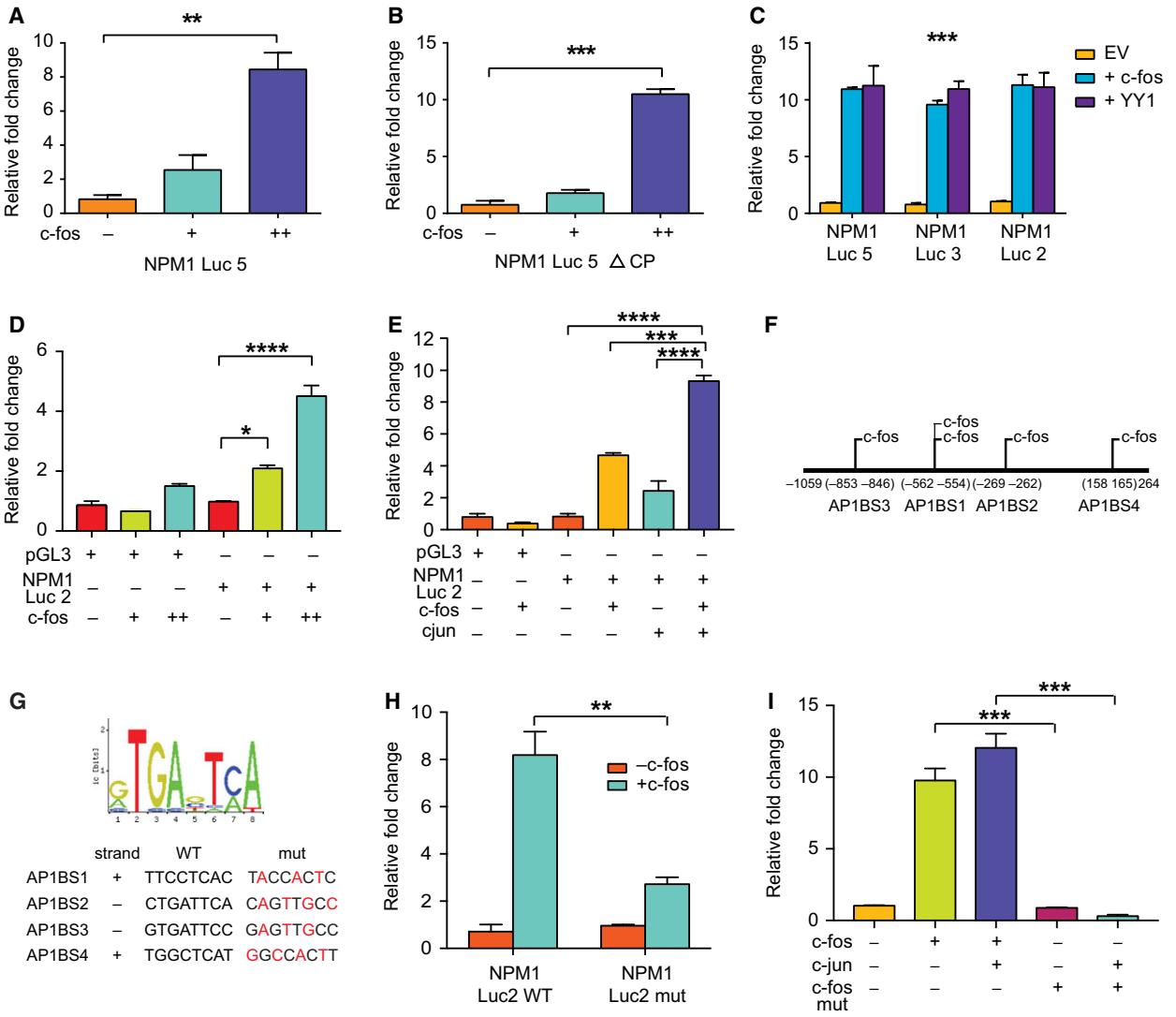

Fig. 2. Transcription factor c-fos activates promoter activity of NPM1 gene by binding to AP-1-binding sites on the promoter. (A,B) Bars represent fold change in relative Luciferase activity after transfection of (A) NPM1 Luc 5 (−2069/+264) (25 ng) and (B) NPM1 Luc 5 ΔCP (−2069/+1) (25 ng) with c-fos (150 ng or 200 ng) or empty vector (200 ng) as indicated post 24 h of transfection in HEK293 cells. (C) Bars represent fold change in relative Luciferase activity after transfection of NPM1 Luc 5 (−2069/+264), NPM1 Luc 3 (−1587/+264) or NPM1 Luc 2 (−1059/+264) (25 ng) with or without c-fos (200 ng) and YY1 (100 ng) as indicated post 24 h of transfection in HEK293 cells. EV, empty vector. (D) Bars represent fold change in relative Luciferase activity after transfection of NPM1 Luc 2 (−1059/+264) or pGL3 basic vector (200 ng) with or without c-fos (200 ng and 400 ng) post 24 h of transfection in H1299 cells. Fold change is relative to pGL3 and NPM1 Luc2. (E) Bars represent fold change in relative Luciferase activity after transfection of NPM1 Luc 2 (−1059/+264) or pGL3 basic vector (200 ng) with or without c-fos (200 ng) or c-jun (200 ng) or both as indicated post 24 h of transfection in H1299 cells. Fold change is relative to pGL3 and NPM1 Luc2. (F) Schematic representation of NPM1 promoter (−1059 to +264) and the position of c-fos-binding sites identified. (G) c-fos transcription factor-binding matrix from Consite. The bottom panel shows the sequences of the site mutations. Red letters indicate the mutated residues. (H) Bars represent fold change in relative Luciferase activity after transfection of WT NPM1 Luc 2 (−1059/+264) or mutant NPM1 promoter (NPM1 Luc 2 mut) (200 ng) with or without c-fos (400 ng) as indicated post 24 h of transfection in H1299 cells. Fold change is relative to respective -c-fos control. (I) Bars represent fold change in relative Luciferase activity after transfection of WT NPM1 Luc 2 (−1059/+264) (200 ng) with or without c-fos, c-jun or c-fos DNA-binding deficient mutant (c-fos mut) (200 ng) as indicated post 24 h of transfection in H1299 cells. Fold change is relative to -c-fos control (lane1). (A)–(E) and (H)-(I) Data were normalized to internal transfection control β-galactosidase. Values are mean + SEM from two experiments with two technical replicates per experiment. Statistical significance was calculated using Student's *t*-test. *$P < 0.05$, **$P < 0.01$, ***$P < 0.001$, ****$P < 0.0001$.

Table 3. Sequences of the c-fos-binding sites on NPM1 promoter (−1059/+264) as predicted by Consite database at 80% cut-off. Positions are with respect to TSS.

Binding site	Sequence	From	To	Score	Strand
AP1BS3	TTCCTCAC	−853	−846	6.720	−
AP1BS1	CTGATTCA	−562	−555	8.378	+
AP1BS1	TGATTCAG	−561	−554	7.410	−
AP1BS2	TGGCTCAT	−269	−262	7.546	−
AP1BS4	GTGATTCC	158	165	6.331	+

using site-directed mutagenesis method as shown in Fig. 2G. Mutation of four AP-1-binding sites on NPM1 promoter led to a decrease in transactivation of the NPM1 promoter by c-fos (Fig. 2H). However, it did not lead to a complete abolishment of the c-fos mediated activation of NPM1 promoter, which indicated that low-affinity-binding sites of c-fos might contribute to its binding and subsequent transactivation. Next, we also created several point mutations in the DNA-binding domain of c-fos targeting mainly the basic residues, namely K153Q, R155Q, R157Q, R158Q, and R159Q that are important for its DNA-binding activity. Additionally, we mutated critical residues in its leucine zipper region, L179V, L186A, and L193V that are essential for its dimerization with c-jun [44]. The mutant c-fos was unable to activate NPM1 promoter activity as compared to the WT c-fos (Fig. 2I), which confirms that c-fos directly binds to the NPM1 promoter to enhance its expression. Furthermore, c-fos transfection in H1299 cells led to a significant increase in NPM1 mRNA (Fig. 3A) as well as protein levels (Fig. 3B). A similar increase in NPM1 mRNA (Fig. 3C) and protein levels (Fig. 3D) was observed upon co-transfection of c-fos and c-jun (AP-1) as well. Appreciable increase in NPM1 protein levels were achieved after transfection of higher doses of c-fos or AP-1 (1.5 μg) as compared to that required to observe upregulation at mRNA levels (500 ng of c-fos or AP-1). The discordance in the degree of upregulation induced by c-fos or AP-1 transfection could be due to the different doses of transfection. However, we do not exclude the possibility of stabilization of NPM1 protein levels by c-fos. To show that c-fos enhances NPM1 transcription by directly binding to the endogenous NPM1 promoter, we performed chromatin immunoprecipitation (ChIP) assays in cells transfected with c-fos. We found that c-fos occupancy was significantly increased at three tested *in silico* identified c-fos-binding sites (Fig. 3E–H). In addition, c-fos occupancy also increased at three other upstream regions that were previously shown to be occupied by c-fos in human cancer cell lines by ENCODE consortium (Fig. 3I–K) [45]. c-fos occupancy was not observed at a negative control region and did not change significantly after c-fos transfection (Fig. 3L). These results show that c-fos/AP-1 indeed activate NPM1 expression in cells.

c-fos and NPM1 expression correlate well in OSCC cells

We next investigated whether NPM1 is overexpressed in oral tumors showing c-fos overexpression. Immunohistochemistry (IHC) analysis of oral tumor tissue array prepared from samples collected from local clinics, re-confirmed the previous results that NPM1 and c-fos are overexpressed in human oral tumor samples when compared to adjacent normal tissues (Fig. 4A–C). Moreover, c-fos expression in individual tumor samples correlated significantly ($r^2 = 0.49$) with NPM1 expression (Fig. 4D). To further evaluate whether c-fos is involved in NPM1 overexpression in OSCC, we tested the effects of c-fos knockdown on NPM1 expression in an oral cancer cell line UPCI:SCC-29B. We used siRNA against c-fos as well as a scrambled siRNA control and measured NPM1 mRNA and protein levels. We achieved ~75% knockdown efficiency with c-fos siRNA (Fig. 4E) as compared to scrambled siRNA control. NPM1 mRNA and protein levels decreased significantly after c-fos knockdown (Fig. 4F, G). We also tested c-fos and c-jun (AP-1) knockdown and observed that NPM1 mRNA and protein levels significantly decreased after knockdown of c-fos and c-jun (Fig. 4H–K). These results indicate that the transcription factor AP-1 is involved in NPM1 overexpression in oral carcinoma.

Since, p53 mutation or loss has been reported to be the cause of 50% of human cancers, we also tested the expression of p53 in the oral tumor tissue arrays with NPM1 and c-fos overexpression. Mutant p53 lose their regulation by Mouse Double Minute 2 (MDM2) and are often overexpressed in tumor cells whereas WT p53 levels are low in normal and tumor cells [46]. Some of these mutants have novel functions distinct from the WT protein that help tumor growth, hence, known as gain-of-function mutants [47]. Interestingly, we found distinct staining pattern of p53 only in a few cells in the section implying the presence of a mutant form of p53 [48] (Fig. 4A). When we compared the expression levels of p53 with that of NPM1 in the oral tumor samples, we found that tumor samples showing positive staining for p53 expression (p53 High) had higher NPM1 levels (Fig. 4L and M) as compared to those with negative or lesser staining for p53 expression (p53 Low), indicating a positive correlation

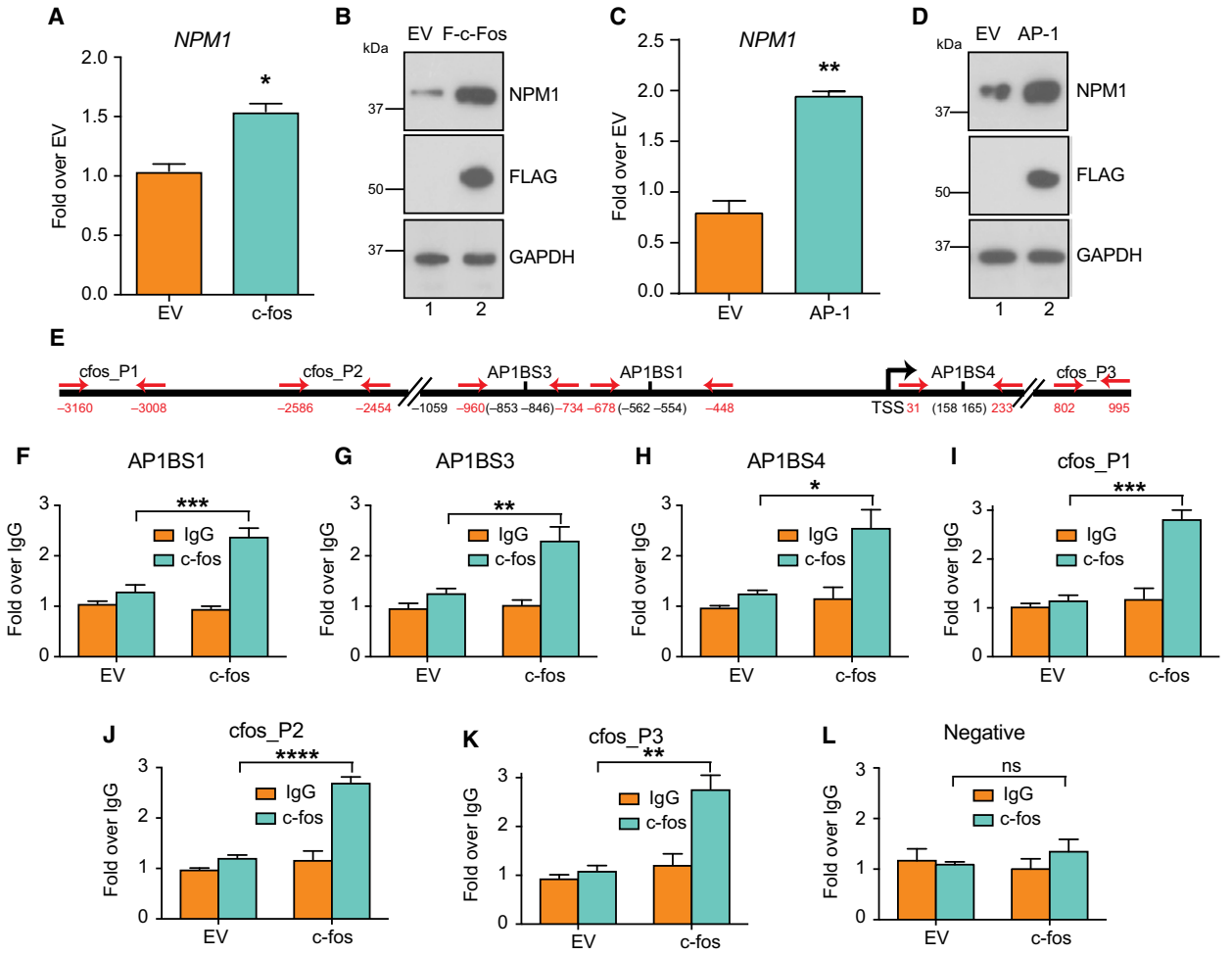

Fig. 3. c-fos and AP-1 (c-fos/c-jun heterodimer) regulate NPM1 expression. (A, C) Bars represent fold change in NPM1 mRNA levels as analyzed by RT-qPCR upon transfecting 500 ng (A) c-fos and (C) AP-1 (c-fos and c-jun; 250 ng each) as indicated, for 24 h in H1299 cells. Internal normalization was done with housekeeping gene β-actin levels. Values are mean+SEM from three independent experiments. Statistical significance was calculated using Student's *t* test. $*P < 0.05$, $**P < 0.01$. (B, D) Western blot analysis after transfection of H1299 cells with 1.5 μg (B) c-fos or (D) c-fos and c-jun (AP-1) (750 ng each) as indicated, for 24 h in H1299 cells. Upper panel shows western blot with anti-NPM1, middle panel with anti-FLAG and bottom panel with anti-GAPDH antibody. F-c-fos: FLAG-c-fos. (E) Schematic showing the position of AP-1-binding sites and the primers used for ChIP experiments. Primer positions are indicated in red. Figure is not drawn to scale. (F–K) c-fos occupancy determined by ChIP-qPCR at various c-fos/AP-1-binding sites on the NPM1 promoter. (L) c-fos occupancy determined by ChIP-qPCR at a negative control region with no c-fos binding. Bars represent the fold enrichment over IgG pulldown in empty vector and c-fos transfected cells. Values are mean + SEM from three independent experiments. Statistical significance was calculated using one-way ANOVA, Tukey's multiple comparisons test. $*P < 0.05$, $**P < 0.01$, $***P < 0.001$, $****P < 0.0001$. EV: empty vector.

between NPM1 and p53 expression in tumor tissues from patient samples.

p53 and NPM1 proteins have been shown to interact with each other, leading to an array of consequences. Most notably, NPM1 enhances transcriptional activation by p53 [49] as well as stabilizes p53 by interacting with MDM2 [50]. However, another group has shown that NPM1 is an early responder to DNA damage that prevents premature activation of p53 [51]. Although numerous studies have implicated NPM1 in the p53 pathway [52–54], no report exists regarding the transcriptional regulation of NPM1 gene either by wild-type p53 or mutant p53 proteins. These facts along with our finding of the positive correlation between NPM1 and p53 expression in oral tumor tissue samples encouraged us to investigate the role of p53 and its mutants in transcriptional regulation of NPM1 expression. Therefore, we first checked whether WT p53 had any influence on NPM1 gene expression.

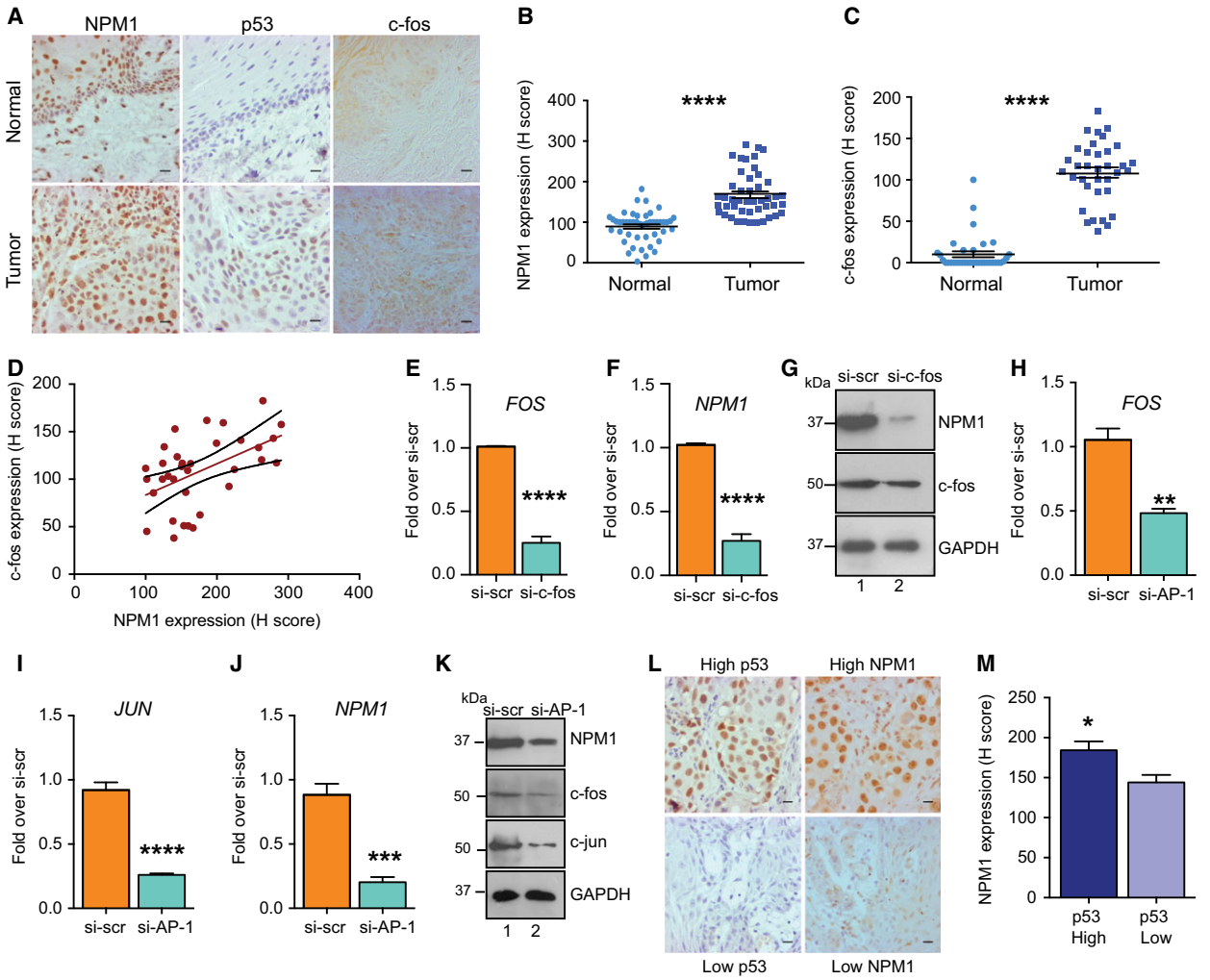

Fig. 4. Nucleophosmin, p53, and c-fos are over-expressed in oral tumor samples. (A) Representative immunohistochemical images of NPM1, p53 and c-fos expression in normal (upper panel) and oral cancer (lower panel) tissue samples. Scale bar is 50 μm. (B) Statistical analysis of NPM1 expression (H-score) between normal and oral cancer samples $n = 46$, $^{****}P < 0.0001$, Mann–Whitney test. (C) Statistical analysis of c-fos expression (H-score) between normal and cancer samples $n = 35$, $^{****}P < 0.0001$, Mann–Whitney test. (D) Correlation of NPM1 and c-fos expression in oral cancer samples (Spearman's correlation coefficient $r^2 = 0.49$, $^{**}P = 0.003$). (E,F) Bars represent fold change in (E) c-fos and (F) NPM1 mRNA levels as analyzed by RT-qPCR upon transfecting 30 nM si-RNA against human c-fos (si-c-fos) or scrambled negative control (si-scr) for 48 h in UPCI:SCC-29B cells. Internal normalization was done with 18S rRNA levels. Values are mean+SEM from four independent experiments. Statistical significance was calculated using Student's *t* test, $^{****}P < 0.0001$. (G) Western blot analysis after transfection of UPCI:SCC-29B cells with 30 nM si-c-fos or si-scr for 48 h. Upper panel shows western blot with anti-NPM1, middle panel with anti-c-fos and bottom panel with anti-GAPDH antibody. (H-J) Bars represent fold change in (H) c-fos, (I) c-jun and (J) NPM1 mRNA levels as analyzed by RT-qPCR upon transfecting 30 nM each of si-RNA against human c-fos and human c-jun (si-AP-1) or 60 nM of si-scr for 48 h in UPCI:SCC-29B cells. Internal normalization was done with 18S rRNA levels. Values are mean + SEM from four independent experiments. Statistical significance was calculated using Student's *t* test, $^{**}P < 0.01$, $^{***}P < 0.001$, $^{****}P < 0.0001$. (K) Western blot analysis after transfection of UPCI:SCC-29B cells with 30 nM each of si-c-fos and si-c-jun (si-AP-1) or 60 nM of si-scr for 48 h. Upper panel shows western blot with anti-NPM1, second panel from top, with anti-c-fos, third panel from top, with anti-c-jun and bottom panel with anti-GAPDH antibody, respectively. (L) Immunohistochemical images of NPM1 and p53 expression in representative high p53 (upper panel) and low p53 (lower panel) expressing tumor samples. Scale bar is 50 μm. (M) Relative expression (H-score) of NPM1 in oral cancer samples showing high and low p53 expression $^{*}P = 0.01$, Mann–Whitney test.

WT p53 does not alter NPM1 transcript levels

Since we were interested in studying the transcriptional regulation of NPM1 by p53, we checked for presence of p53-binding sites on NPM1 promoter, using Consite database. We found several low-scoring putative p53-binding sites in the 7 kb sequence (−6 kb/+1 kb) of

the NPM1 promoter region (eleven sites at 60% cut off; data not shown). Transcriptional effect of p53 on endogenous NPM1 expression was investigated by expressing WT p53 in H1299 p53 null cells. WT p53 expression did not significantly alter the NPM1 transcript levels (Fig. 5A) although p53 protein was highly expressed after transfection (Fig. 5B). In an alternate approach, human colorectal carcinoma cells, HCT116 $p53^{+/+}$, expressing WT p53 were treated with increasing doses of Nutlin-3a, an MDM2 inhibitor that stabilizes p53 protein and enhances its level in cells. NPM1 transcript levels did not alter significantly upon Nutlin-3a treatment (Fig. 5C) whereas the known p53 responsive gene p21 or cyclin-dependent kinase inhibitor 1A (CDKN1A) levels increased significantly as expected in a dose-dependent manner under the same conditions (Fig. 5D) showing that indeed p53 protein levels were upregulated. These results show that WT p53 does not transcriptionally alter NPM1 levels. This observation was explained by the absence of high-scoring p53-binding sites in the NPM1 promoter sequence as analyzed and mentioned earlier. NPM1 protein levels were also checked by western blot analysis upon treatment with increasing doses of Nutlin-3a for 6 and 12 h. There was no significant alteration observed in the NPM1 protein levels upon treatment with Nutlin-3a (Fig. 5E, compare lanes 3–6 versus lanes 1 and 2 and Fig. 5F).

Mutant p53 (R175H) enhances NPM1 expression

Our observation of WT p53 not significantly regulating NPM1 expression, does not eliminate the possibility of the role of p53 mutants in this process, given the fact that many hot-spot p53 mutants act in a gain-of-function manner regulating specific sets of genes by their unique mechanisms which are different from that of WT p53 [47,55]. Hence, to test this hypothesis, we checked whether mutant p53 could activate NPM1 expression. p53 has six hotspot residues that are frequently mutated in all types of cancer. Among these, R175H is the most frequent mutation and it is the fourth frequent mutation across all cancer types considering all gene mutations [55]. R175H is a gain-of-function conformational mutant of p53 that does not bind to DNA without the help of accessory factors. Hence, we first tested the effect of R175H p53 expression on NPM1 promoter activity. Co-transfection of NPM1 promoter NPM1 Luc 2 (−1059/+264) with R175H p53 expression plasmid led to an increase

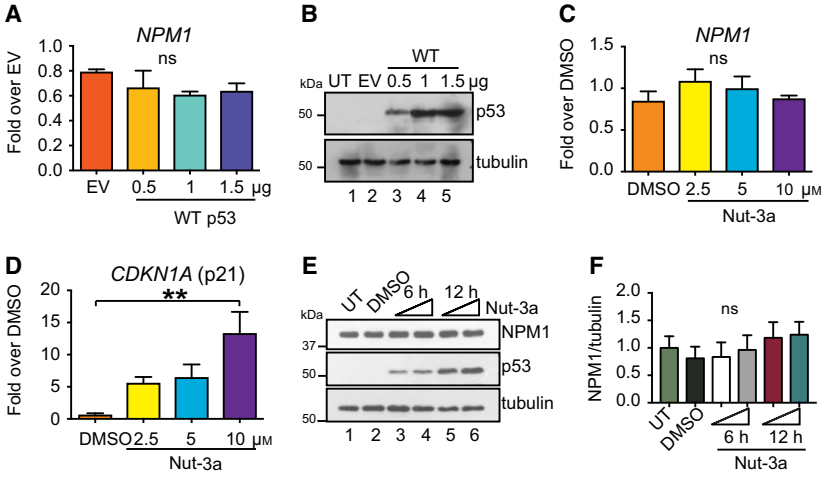

Fig. 5. Wild-type p53 does not regulate NPM1 expression. (A) Bars represent fold change in NPM1 mRNA levels as analyzed by RT-qPCR upon transfecting different doses of WT p53 as indicated for 24 h in H1299 $p53^{-/-}$ cells. Internal normalization was done with housekeeping gene β-actin levels. Values are mean+SEM from two independent experiments and three technical replicates from each experiment. Statistical significance was calculated using Student's *t* test. ns: non-significant, EV: empty vector. (B) Western blot analysis after transfection of different doses of WT p53 as indicated for 24 h in H1299 cells. Upper panel shows western blot with anti-p53 and lower panel shows western blot with anti-tubulin antibody. (C,D) Bars represent fold change in (C) NPM1 and (D) p21 mRNA levels as analyzed by RT-qPCR upon treatment with different doses of Nutlin-3a for 24 h in HCT116 $p53^{+/+}$ cells as indicated. Internal normalization was done with housekeeping gene β-actin levels. Values are mean + SEM from three independent experiments. Statistical significance was calculated using Student's *t* test. $^{**}P < 0.01$, ns: non-significant. (E) Western blot analysis after treatment of HCT116 $p53^{+/+}$ cells with 5 µM (lanes 3 and 5) and 10 µM (lanes 4 and 6) of Nutlin-3a (Nut-3a) for 6 (lanes 3 and 4) and 12 h (lanes 5 and 6). Upper panel shows western blot with anti-NPM1, middle panel with anti-p53 and bottom panel with anti-tubulin antibody. (F) Densitometric quantification of NPM1 protein expression normalized to tubulin using values from three independent experiments. ns: non-significant.

in the NPM1 promoter activity in a dose-dependent manner (Fig. 6A). R175H p53 transfection in H1299 cells resulted in a significant increase in NPM1 mRNA (Fig. 6B) and protein levels (Fig. 6C). Moreover, R175H overexpression in a p53 null oral cancer cell line UM-SCC-1 induced NPM1 protein levels as well

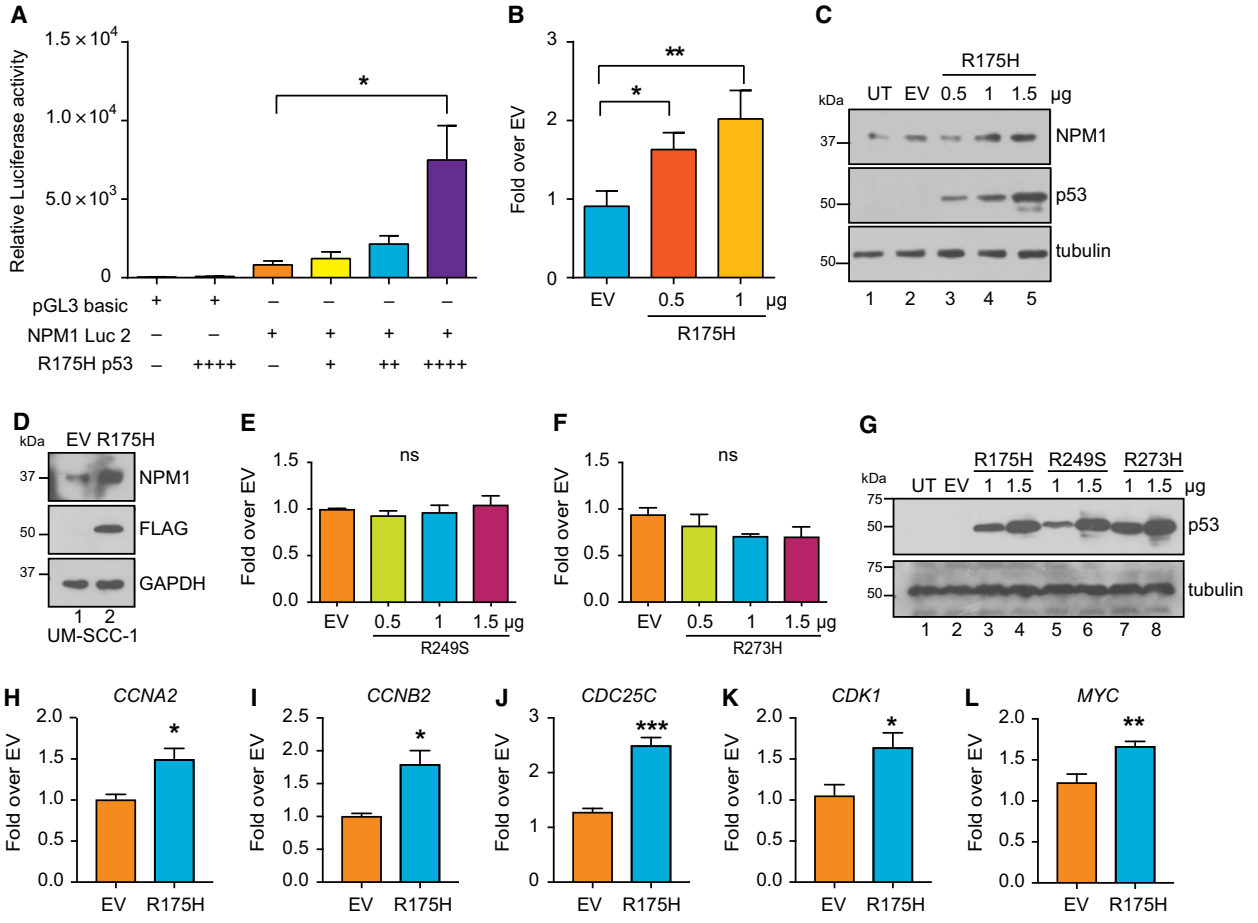

Fig. 6. Mutant p53 (R175H) enhances NPM1 expression. (A) Bars represent relative Luciferase activity after transfection of pGL3 basic vector or NPM1 Luc 2 (−1059/+264) (200 ng) with R175H mutant p53 (100 ng, 200 ng or 400 ng) or empty vector (pGL3 basic, 400 ng) as indicated post 24 h of transfection in H1299 cells. Data were normalized to internal transfection control β-galactosidase. Values are mean + SEM from two experiments and two technical replicates in each experiment. Statistical significance was calculated using One-way ANOVA, Tukey's multiple comparisons test. $*P < 0.05$. (B) Bars represent fold change in NPM1 mRNA levels as analyzed by RT-qPCR upon transfecting different doses of R175H mutant p53 as indicated for 24 h in H1299 cells. Internal normalization was done with housekeeping gene β-actin levels. Values are mean+SEM from three independent experiments. Statistical significance was calculated using Student's *t* test. $*P < 0.05$, $**P < 0.01$ (C) Western blot analysis after transfection of H1299 cells with indicated amounts of R175H mutant p53 expression construct for 24 h. Upper panel shows western blot with anti-NPM1, middle panel with anti-p53 and bottom panel with anti-tubulin antibody. (D) Western blot analysis after stable constitutive expression of empty vector (EV) or FLAG tagged R175H p53 in UM-SCC-1 $p53^{-/-}$ oral cancer cells. Upper panel shows western blot with anti-NPM1, middle panel with anti-FLAG and bottom panel with anti-GAPDH antibody. (E,F) Bars represent fold change in NPM1 mRNA levels as analyzed by RT-qPCR upon transfecting different doses of (E) R249S and (F) R273H mutant p53 as indicated for 24 h in H1299 cells. Internal normalization was done with housekeeping gene β-actin levels. Values are mean + SEM from two independent experiments and three technical replicates from each experiment. Statistical significance was calculated using Student's *t* test. EV, Empty vector; ns, non-significant. (G) Western blot analysis after transfection of different doses of R175H, R249S and R273H mutant p53 for 24 h in H1299 cells as indicated. Upper panel shows western blot with anti-p53 and bottom panel shows western blot with anti-tubulin. EV, empty vector; UT, untransfected. (H–L) Bars represent fold change in (H) CCNA2 (I) CCNB2 (J) CDC25C (K) CDK1 and (L) c-MYC mRNA levels as analyzed by RT-qPCR upon transfecting 500 ng of R175H mutant p53 or empty vector as indicated for 24 h in H1299 cells. Internal normalization was done with housekeeping gene β-actin levels. EV, empty vector. Values are mean + SEM from two independent experiments and three technical replicates from each experiment. Statistical significance was calculated using Student's *t* test. $*P < 0.05$, $**P < 0.01$, $***P < 0.001$.

(Fig. 6D). These results show that R175H p53 indeed transcriptionally activates NPM1 expression in cells. However, the mechanism of R175H-mediated transactivation of NPM1 expression is unclear. We also screened a few other hot-spot mutants of p53 such as R249S and R273H p53. None of these mutants could induce NPM1 transcript levels (Fig. 6E and F) even when similar levels of protein expression were achieved for each mutant after transfection (Fig. 6G) implying that the effects of R175H p53 on NPM1 expression were specific to this mutant. Since these mutants did not enhance NPM1 transcript levels, we did not further check NPM1 protein levels as we were particularly interested in investigating the transcriptional regulation of NPM1 by mutant p53. We subsequently validated the expression of some of the known targets of R175H p53. Expression of important cell cycle genes such as cyclin A2 (CCNA2), cyclin B2 (CCNB2), cell division cycle 25C (CDC25C), and cyclin-dependent kinase 1 (CDK1) were enhanced by overexpression of R175H p53 as was reported earlier [55] (Fig. 6H–K). Interestingly, these genes are targets of the nuclear transcription factor Y (NF-Y) as well. R175H p53 was previously reported to interact with NF-Y and induce the expression of these NF-Y target genes [47]. Additionally, we also observed that c-myc mRNA levels were enhanced upon R175H expression in H1299 cells as reported earlier [56] (Fig. 6L). Presumably, the increased expression of all these genes along with NPM1 contribute collectively to the process of tumorigenesis.

c-fos interacts with and recruits R175H to NPM1 promoter

Given that c-fos and R175H p53 transcriptionally activate NPM1 expression and R175H itself is unable to bind to the DNA to cause gene transactivation, we tested if c-fos and R175H could interact, leading to recruitment of mutant p53 to the NPM1 promoter. Co-immunoprecipitation results showed that mutant p53 was pulled down with FLAG-c-fos in H1299 cells co-transfected with R175H p53 and FLAG-c-fos (Fig. 7A), indicating that these two proteins interact. Moreover, c-fos and R175H p53 seem to colocalize in the nucleus as observed by co-immunofluorescence analyses (Fig. 7B). In addition, we performed co-immunoprecipitation assays with R249S and R273H to evaluate whether the interaction with c-fos was specific to R175H p53. Results showed that R249S and R273H also bind to c-fos which might be artificially induced due to overexpression of both proteins (Fig. 7C). To evaluate whether c-fos binds to R175H at endogenous levels, we performed the co-immunoprecipitation experiment in AU565 cell line which contains naturally mutated R175H p53. Results showed that R175H p53 is indeed pulled down with c-fos immunoprecipitation indicating that R175H p53 indeed binds to c-fos (Fig. 7D). Next, in order to study the effect of R175H overexpression on the endogenous c-fos binding on NPM1 promoter, we made a stable cell line with doxycycline-inducible expression of R175H p53. We confirmed the doxycycline-induced expression of FLAG-tagged R175H p53 using immunofluorescence and western blot assays (Fig. 7E and F). Doxycycline-induced expression of R175H enhanced NPM1 expression at both protein (Fig. 7F) and RNA levels (Fig. 7G). c-fos transcript levels were not significantly altered by the induction of R175H expression, indicating that R175H does not have a direct effect on the levels of c-fos itself (Fig. 7H). However, R175H overexpression enhanced the occupancy of c-fos on NPM1 promoter at the c-fos/AP-1-binding sites as observed by ChIP assays (Fig. 8A–F). Interestingly, R175H itself was recruited at the AP-1-binding sites upon doxycycline-mediated induction (Fig. 8G and H). In accordance with previous reports [55], we also validated the enrichment of R175H p53 at known target promoters of the cell cycle genes CCNA2, CDC25C and CDK1 by ChIP assays (Fig. 8I–K). To investigate whether the presence of R175H p53 affects the induction of NPM1 expression by c-fos, we tested NPM1 expression levels with c-fos overexpression with or without doxycycline treatment. Results showed that in the presence of R175H p53, c-fos overexpression led to highest amount of NPM1 protein expression (Fig. 8L, compare lanes 2 versus 4). c-fos and R175H p53 were individually able to induce NPM1 levels although at lower levels than when present together (Fig. 8L). Altogether, these results show that R175H might induce c-fos recruitment to the NPM1 promoter by an unknown mechanism and c-fos, in turn, could recruit R175H p53 to the NPM1 promoter, thereby enhancing NPM1 expression levels.

Discussion

Nucleophosmin is frequently overexpressed in several types of solid tumors. However, the mechanisms driving the increased expression of NPM1 are largely unknown. Here, we show that c-fos and R175H p53 activate NPM1 gene expression at the transcript level that was consistent at the protein levels as well. c-fos forms heterodimer with c-jun through their leucine zipper domains forming the AP-1 transcription factor complex that binds to AP-1 target sites. NPM1

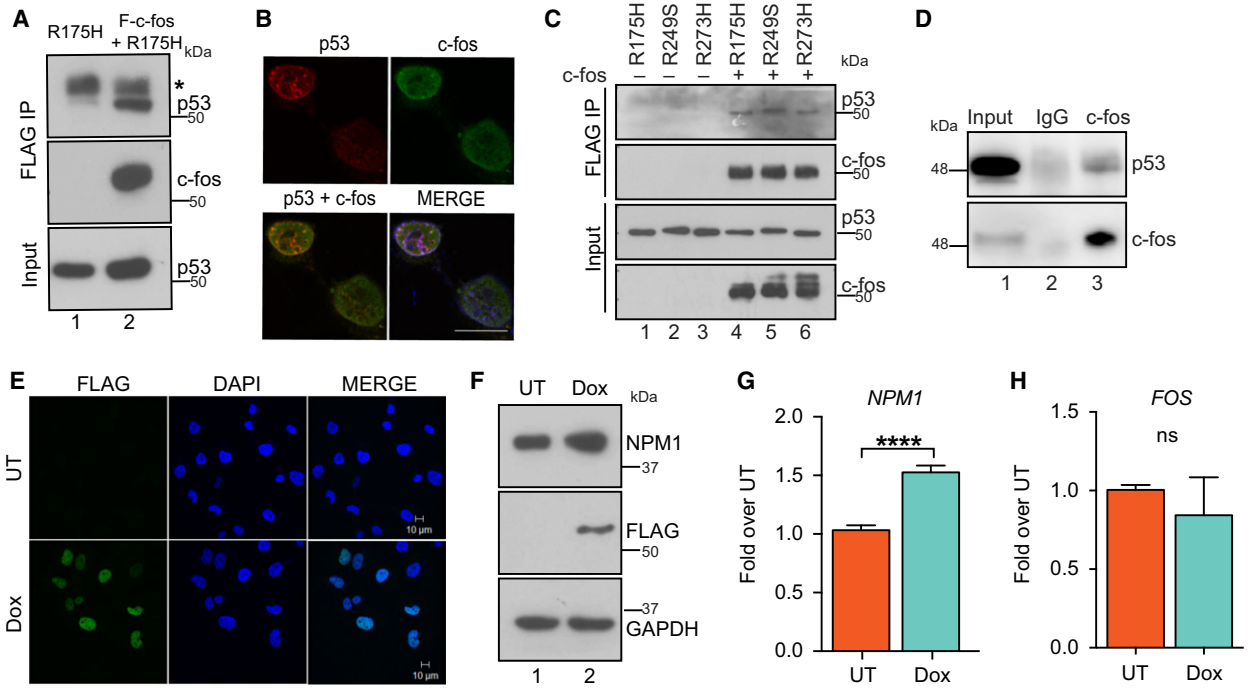

Fig. 7. R175H mutant p53 and c-fos interact. (A) Western blot analysis after anti-FLAG immunoprecipitation in H1299 cells transfected with either R175H mutant p53 and empty vector (5 µg each) or R175H mutant p53 and FLAG c-fos (5 µg each) co-transfection for 24 h. Upper panel shows western blot with anti-p53, middle panel with anti-c-fos in IP eluates and bottom panel with anti-p53 antibody in input lysates. Asterisk (*) indicates the antibody heavy chain band. Input was 1% of the lysate used for immunoprecipitation. (B) Co-immunofluorescence analysis of cellular localization of R175H mutant p53 (in red) and c-fos (in green) after transfection of 700 ng each of R175H mutant p53 and c-fos in H1299 cells for 24 h. Nuclei were stained with Hoechst. Yellow pixels in the merged panel indicate colocalization of R175H mutant p53 and c-fos in the nuclei of the cells. Scale bar is 20 µm. (C) Western blot analysis after anti-FLAG immunoprecipitation in H1299 cells co-transfected separately with R175H, R249S and R273H mutant p53 (2 µg each) with empty vector (2 µg) or FLAG c-fos (2 µg) for 24 h. Upper panel and third panel from top show western blot with anti-p53, bottom panel and second panel from top show western blot with anti-c-fos. Input was 1% and 3% of the lysate used for immunoprecipitation for western blot with anti-p53 and anti-c-fos, respectively. (D) Western blot analysis after c-fos immunoprecipitation from AU565 cell lysates for p53 (upper panel) and c-fos (lower panel). Input was 1% and 5% of the lysate used for immunoprecipitation for p53 and c-fos blots, respectively. (E) Immunofluorescence analysis of 3X-FLAG R175H mutant p53 expressing H1299 cells induced with 1 µg·mL^{-1} doxycycline (Dox) for 72 h or left uninduced (UT) using anti-FLAG antibody. Nuclei were stained with Hoechst. Scale bar is 10 µm. (F) Western blot analysis showing increase in NPM1 protein levels (upper panel) after induction of R175H by doxycycline treatment. GAPDH (bottom panel) serves as loading control. anti-FLAG (middle panel) shows expression of 3X-FLAG-R175H mutant p53. (G,H) Bars represent fold change in (G) NPM1 and (H) c-fos mRNA levels as measured by RT-qPCR after R175H mutant p53 induction by doxycycline treatment. Values are mean + SEM from three independent experiments. Statistical significance was calculated using Student's *t* test. ****$P < 0.0001$, ns, non-significant.

promoter harbors multiple AP-1 target sites and our data suggest that AP-1 indeed enhances NPM1 gene expression which is relevant in the context of cancer. Further, R175H, a gain-of-function mutant of p53 that has been implicated in the tumorigenesis in several cancers, was also found to have a positive effect on NPM1 expression. The expression of this mutant in cells leads to increase in proliferation, invasion and migration [53]. It is also shown to activate expression of several cell-cycle-related genes such as CCNA2, CCNB2, CDK1 and CDC25C [47,55]. These genes are targets of transcription factor NF-Y, and R175H has been reported to interact with NF-Y leading to recruitment of R175H to NF-Y target genes with the concomitant transactivation of these genes. Besides NF-Y, R175H also binds to several transcription factors such as Specificity protein 1 (Sp1), nuclear factor kappa B (NF-κB) and vitamin D receptor (VDR) [47]. NPM1 promoter contains binding sites for all the above-mentioned transcription factors, and hence, R175H could potentially bind to any one or more of these factors and get recruited onto NPM1 promoter. In

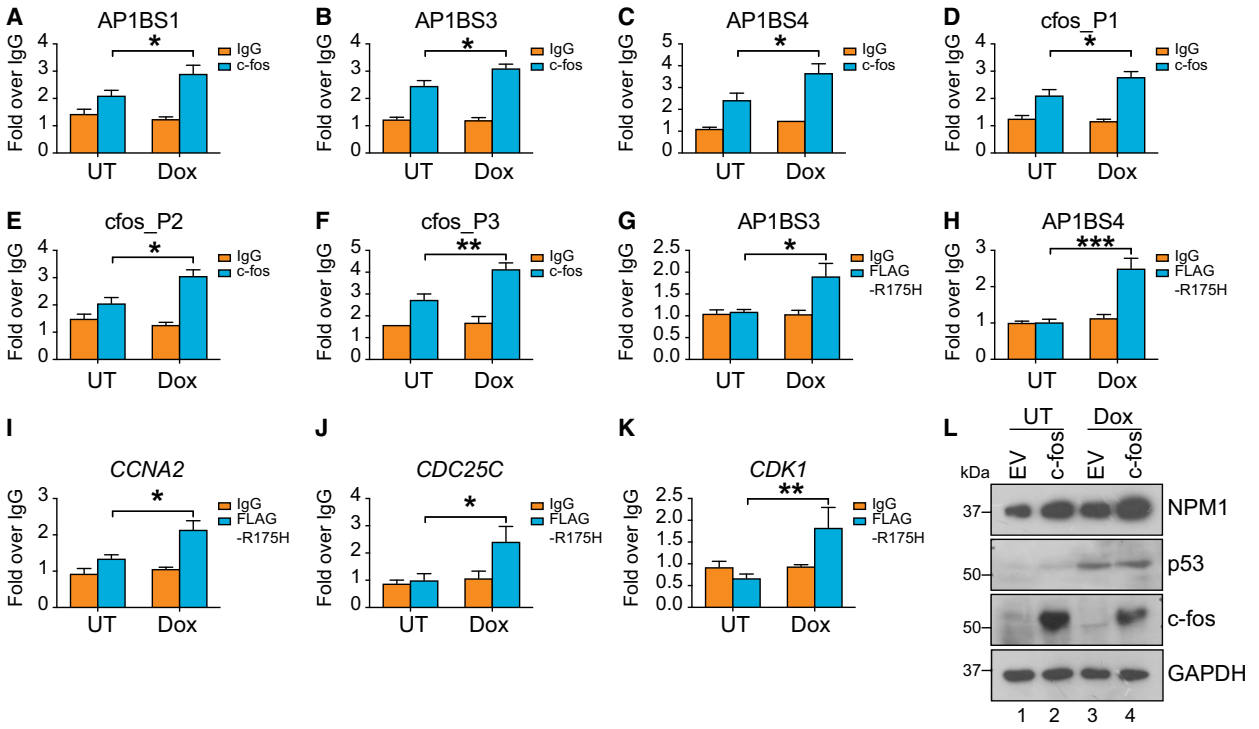

Fig. 8. R175H mutant p53 and c-fos synergistically enhance recruitment of each other in an auto-feedback loop. (A–F) c-fos occupancy determined by ChIP-qPCR at various c-fos/AP-1-binding sites on the NPM1 promoter. Bars represent the fold enrichment over IgG pulldown in untreated (UT) and doxycycline (Dox)-treated cells. Values are Mean+SEM from two independent experiments and three technical replicates from each experiment. (G–K) FLAG-R175H occupancy determined by ChIP-qPCR at (G,H) c-fos-binding sites on NPM1 promoter and (I–K) on positive control gene promoters as indicated. Bars represent the fold enrichment over IgG pulldown in untreated (UT) and doxycycline (Dox)-treated cells. Values are mean + SEM from two independent experiments and three technical replicates from each experiment. Statistical significance was calculated using one-way ANOVA, Tukey's multiple comparisons test. $*P < 0.05$, $**P < 0.01$, $***P < 0.001$. (L) Western blot analysis after transfection of c-fos (1.5 μg) or empty vector (1.5 μg) with or without R175H mutant p53 induction by doxycycline treatment (1 $\mu g \cdot mL^{-1}$) as indicated for 24 h in H1299 cells. Upper panel shows western blot with anti-NPM1, second panel from top, with anti-p53, third panel from top, with anti-c-fos and bottom panel with anti-GAPDH antibody, respectively.

addition, R175H induces expression of several transcription factors such as MYC proto-oncogene (c-myc), early growth response 1 (EGR1) and nuclear factor kappa B subunit 2 (NF-κB2) [47]; hence R175H could activate these and induce NPM1 expression. R175H is also known to interact with co-activator CREB-binding protein (CBP)/p300 through its transactivation domain [47,57]. NPM1 is a reported target of c-myc which gets induced by R175H. Hence there could be multiple possible mechanisms of regulation of NPM1 expression by R175H, and it needs to be confirmed which of these mechanisms or a combination of them is at play. Interestingly, NPM1 has been reported earlier to enhance the stability of R175H and R248W p53 mutants [46] suggesting that there could be a positive feed-back loop connecting these players in promoting tumor progression. Our study suggests the involvement of c-fos as a novel factor regulating NPM1 expression. We also observe an additional synergistic effect of both c-fos and R175H p53 in enhancing NPM1 expression. The overexpression of c-fos and mutant p53 along with NPM1 in oral cancer patient tissues suggests the possible existence of this molecular pathway at the physiological level. The reported overexpression of c-fos and mutant p53 in melanoma [58] also supports this view. Although in our studies, another conformational mutant R249S and a DNA contact mutant R273H did not seem to affect NPM1 expression, we cannot rule out the possibility that other p53 mutants that are functionally similar to R175H, might regulate NPM1 expression.

Materials and methods

Cell culture

Human cell lines, HEK293 (CRL-1573), NCI-H1299 (CRL-5803), HCT116p53$^{+/+}$ (CCL-247), AU565 (CRL-2351)

were purchased from American Type Culture Collection (ATCC, Manassas, VA, USA). UPCI:SCC-29B and UM-SCC-1 cells were kind gifts from Prof. Susanne M. Gollin (University of Pittsburgh) and Dr. Gautam Sethi (National University of Singapore), respectively. HEK293 and UM-SCC-1 cells were grown in Dulbecco's modified Eagle's medium (DMEM) (Gibco, Carlsbad, CA, USA), H1299 and AU565, in RPMI-1640 (Gibco), SCC-29B, in Minimum essential medium (MEM) (Gibco) and HCT116p53$^{+/+}$ cells, in Mc-Coy's-5a medium (Gibco) at 37 °C, 5% CO_2 in a humidified chamber. The H1299 cells stably harboring the 3xFLAG-R175H p53 in pEBTetD vector were grown in media containing 1.1 $\mu g \cdot mL^{-1}$ of Puromycin dihydrochloride (Sigma, St. Louis, MO, USA) antibiotic. The UM-SCC-1 cells stably harboring the 3xFLAG-R175H p53 in p3xFLAG-CMV10 vector were grown in media containing 0.4 $mg \cdot mL^{-1}$ of G418 disulfate salt (Sigma) antibiotic. All the media were supplemented with 10% Fetal Calf Serum (v/v) (Gibco) and 1X antibiotics containing penicillin, streptomycin, and amphotericin (Hi-Media, Mumbai, Maharashtra, India). All cell lines used in this study were tested and found to be mycoplasma negative.

Plasmids

Human genomic DNA was isolated from the blood sample of a healthy individual at Dhanvantari Clinic at JNCASR after obtaining informed consent from the individual, using the Genomic DNA isolation kit (Sigma-Aldrich, St. Louis, MO, USA). The different NPM1 promoter fragments were amplified from this human genomic DNA by PCR using specific primers listed in Table 4. The fragments were cloned between the *Kpn* I and *Xho* I sites of the pGL3 basic vector (Promega, Madison, WI, USA). The c-fos/AP-1-binding sites on the NPM1 Luc 2 (−1059 to +264) plasmid were mutated using the QuikChange II XL Site-Directed Mutagenesis Kit (Stratagene, La Jolla, CA, USA). The full-length c-fos coding sequence was amplified from HEK293 cDNA using specific primers (Table 4) and cloned into the *Hind* III and *Xba* I sites of the pFLAG-CMV2 vector (Sigma) resulting in an N-terminal FLAG-tagged c-fos construct. The c-fos DNA-binding-deficient mutants were generated by site-directed mutagenesis of FLAG-c-fos plasmid. The c-jun expression plasmid was a kind gift from Dr. Sagar Sengupta (National Institute of Immunology, India). The wild-type p53 (pCMV-wtp53) expression plasmid was a kind gift from Prof. Bert Vogelstein (Johns Hopkins University, Baltimore, MD, USA). The WT p53 coding sequence was amplified by PCR from a pCMV-wtp53 template using specific primers (Table 4) and cloned into the *Hind* III and *Bam* HI sites of the pFLAG-CMV2 and p3XFLAG-CMV-10 vector (Sigma) resulting into N-terminal FLAG-tagged and 3X-FLAG tagged p53 expression constructs. The gain of function (GOF) p53 mutants R175H, R273H, and R249S expression constructs were generated by site-directed mutagenesis of FLAG-WT p53 using the QuikChange II XL Site-Directed Mutagenesis Kit (Stratagene). The 3X-FLAG-R175H construct was generated similarly by site-directed mutagenesis of 3X-FLAG-WT p53 construct. The primer sequences used for various point mutants have been listed in Table 4. The inducible R175H p53 expression constructs were generated by subcloning the WTp53 and R175Hp53 amplicons into the pEBTetD vector; pEBTetD SLC22A1 vector was a kind gift from Dr. Dirk Gründemann (University of Cologne, Germany). The SLC22A1 insert was released by digestion with *Kpn* I and *Xho* I and the R175H p53 insert was cloned into the same site.

All constructs were confirmed by insert release and sequencing.

Transient transfection of plasmid DNA in mammalian cells

HEK293 and H1299 cells were transfected with mammalian expression plasmids using the Lipofectamine 2000 transfection Reagent (Life Technologies, Carlsbad, CA, USA) according to the manufacturer's instructions.

Generation of stable cell lines

Stable cell lines were generated in UM-SCC-1 by transfecting them with the 3X-FLAG-R175H construct or the empty vector for a period of 24 h followed by selection with 600 $\mu g \cdot mL^{-1}$ of G418 antibiotic over a period of 7 days. Single cell colonies were selected and characterized for expression of 3X-FLAG-R175H protein. Inducible R175H p53 expressing cell lines were generated by transfecting H1299 cells with pEBTetD-R175H construct for a period of 24 h followed by selection with 1.1 $\mu g \cdot mL^{-1}$ of puromycin over a period of 4 days. Single cell colonies were selected and characterized for doxycycline induced expression of 3X-FLAG-R175H protein.

Transient transfection of si-RNA in mammalian cells

si-RNA against human c-fos (Santacruz, Dallas, TX, USA, Cat No. sc-29221, Lot No. C1417), human c-jun (Santacruz, Cat No. sc-29223, Lot No. H3117) and scrambled negative control (Ambion, Cat No. AM4611, Lot No. AS0240KM) were transfected in SCC-29B cells using Lipofectamine RNAiMAX Transfection Reagent (Life Technologies) in 6-well format as per manufacturer's protocol. Transfection was done twice at 24 h interval and cells were harvested after 48 h of first transfection, for analysis of protein and RNA expression.

Table 4. Sequences of primers used in the study.

Construct	Forward primer (5′-3′)	Reverse primer (5′-3′)
Cloning primers		
NPM1 Luc 1 (−668 to +965)	cggggtaccacccgctttctttcaggagg	ccgctcgagacagcatccctggc tcacga
NPM1 Luc 2 (−1059 to +264)	cggggtacccaggagctctcagaaaggaacag	ccgctcgagtgtccatcgaatctt ccatcggg
NPM1 Luc 3 (−1587 to +264)	cggggtacccttttgggaggccaacatggcgaaa	ccgctcgagtgtccatcgaatcttc catcggg
NPM1 Luc 4 (−1059 to +774)	cggggtacccaggagctctcagaaaggaacag	ccgctcgagggctctgaggccagaa taacgc
NPM1 Luc 5 (−2069 to +264)	cggggtacccaaccatatacccatcacccag	ccgctcgagtgtccatcgaatcttc catcggg
NPM1 Luc 2 Δ CP (−1059 to +1)	cggggtacccaggagctctcagaaaggaacag	ccgctcgagacctcgcccccacctc cttcc
NPM1 Luc 3 Δ CP (−1587 to +1)	cggggtacccttttgggaggccaacatggcgaaa	ccgctcgagacctcgcccccacctc cttcc
NPM1 Luc 5 Δ CP (−2069 to +1)	cggggtacccaaccatatacccatcacccag	ccgctcgagacctcgcccccacctc cttcc
FLAG-CFOS	cccaagcttatgatgttctcgggc	gctctagatcacagggccagcag
FLAG-p53	cccaagcttatggaggagccgcagtc	cgcggatcctcagtctgagtcaggc
pEBTetD-R175H-p53	cggggtaccatggactacaaagacgatg	ccgctcgagtcagtctgagtcaggccc
Site-directed mutagenesis primers		
AP1BS1mut	gtccttgctaatttggagacagttgccg tccccttttggcccccaag	cttgggggccaaaaggggacggcaact gtctccaaattagcaaggac
AP1BS2mut	gaatcgaggtgctctcggccactt tcgcagccggctaac	gttagccggctgcgaaagtggccgaga gcacctcgattc
AP1BS3mut	gtcttccttttctgaggctatcatttgt ataccactcttcttaaatt tgtttgatatgt	acatatcaaacaaatttaagaagagt ggtatacaaatgatagcctca gaaaggaagac
AP1BS4mut	gtcctttccctggtgagttgc cgtcctgcgcggtt	aaccgcgcaggacggcaactcacca gggaaaggac
Cfosmut1 (K153Q, R155Q, R157Q, R158Q and R159Q)	gcagcccaatgccaaaaccagcagcagg agctgactgatacactccaag	gctcctgctgctggttttggcattggg ctgcagccatcttattcctttc
Cfosmut2 (L179V, L186A and L193V)	gctgtgcagaccgagattgccaacgcgct gaaggagaaggaaaaag tagagttcatcctg	tacttttttccttctccttcagcgcgtt ggcaatctcggtctgcacagca gacttctcatc
R175H p53	gacggaggttgtgaggcactgccccca ccatgag	ctcatggtgggggcagtgcctcacaa cctccgtc
R273H p53	ggaacagctttgaggtgcatgtttgtgc ctgtcctggg	cccaggacaggcacaaacatgcacct caaagctgttcc
R249S p53	gggcggcatgaaccggagccccatcct caccatc	gatggtgaggatggggctccggttca tgccgccc

Gene	Forward primer (5′-3′)	Reverse primer (5′-3′)
RT-qPCR primers		
NPM1	gttcagggccagtgcatatta	tttctgtggaaccttgctacc
CCNB2	ggctggtacaagtccactcc	gaagccaagagcagagcagt
CCNA2	cgaaagactggatataccctgg	catcttagaaaacaaaggcagtct
CDK1	aacttggatgaaaatggcttgg	aagagttaacaataaaaacacaactatctg
CDC25C	ttctggtgaaggacatgagc	ggcctggatacaagttggtag
CDKN1A/p21	gaacttcgactttctcagcg	tggagtggtagaaatctgtc
MYC	atgtcctgagcaatcacctatg	caaagtccaatttgaggcagtt
ACTB	agatgtggatcagcaagcaggagt	tcctcggccacattgtgaactttg
18S	gtaacccgttgaaccccatt	ccatccaatcggtagtagcg
FOS	gactgatacactccaagcgg	catcagggatcttgcaggc
JUN	tccttaagaacacaaagcggg	acacagttaacgaaggcagg

Table 4. (Continued).

Gene/Binding Site	Forward primer (5′-3′)	Reverse primer (5′-3′)
ChIP primers		
AP1BS1	tcttacaagtcacccgctttc	tgtagttaccggccagactta
AP1BS3	actgttcattcctctcttgatagac	agctacaccttgacaaactcc
AP1BS4	aggacggctacggtacg	acgcacttaggtaggagagaa
CCNA2	gagtcagccttcggacagcc	ccagagatgcagcgagcagc
CDC25C	gaatggacatcactagtaaggcgcg	gcaggcgttgaccattcaaaccttc
CDK1	gaactgtgccaatgctggga	gcagtttcaaactcaccgcg
cfos_P1	gagacgggatttctccatgtt	cattaccttgagtcatgttgtcatt
cfos_P2	acccaggctagagagtagtg	aaattagccgggtgtggtag
cfos_P3	cgtgcttcggccagtta	gcctcttaacatttcccacttc
Negative	cagaaaggaaggagccacaa	tagcagggtgggaactctaa

Luciferase assay

After 24 h of transfection, cells were washed with PBS and lysed in 1X Reporter lysis buffer (Promega) for 20 minutes on ice. The clarified cell lysate was mixed with equal volumes of 2X Luciferase substrate (Promega) and the luciferase counts were measured using a Wallac 1409 liquid scintillation counter (Wellesley, MA, USA). The internal transfection control plasmid used was pCMV-LacZ which expresses β-Galactosidase enzyme from the constitutive CMV promoter. Transfection efficiency across wells was normalized by performing β-Galactosidase assay. Equal volumes of cell lysate and 2X β-Galactosidase substrate were mixed and incubated at 37 °C for 5 minutes (Promega) or until the appearance of yellow color was observed. The reaction was stopped by addition of 1M Na_2CO_3 to a final concentration of 500 mM and the amount of product formed was measured using the VersaMax ELISA reader (Molecular Devices, Sunnyvale, CA, USA).

Drug treatment

HCT116 $p53^{+/+}$ cells were treated with 2.5, 5 or 10 μM Nutlin-3a (Sigma) for 6, 12 or 24 h after which total protein or RNA was extracted from cells for further analyses.

Reverse transcription PCR analysis

Total RNA was extracted from cells using TRIZOL reagent (Invitrogen, Carlsbad, CA, USA) according to the manufacturer's instructions. RNA was treated with DNase I (NEB, Ipswich, MA, USA) according to the manufacturer's instructions followed by re-precipitation. First strand cDNA was synthesized from 2 μg of total RNA using Moloney Murine Leukemia Virus Reverse Transcriptase (Sigma) and oligo dT (Sigma) as per the manufacturer's instructions. Real-time PCR was performed on a Step One Plus Real-Time PCR Detection System [Applied Biosystems (ABI), Waltham, MA, USA] using 2X Power SYBR Green Mastermix (ABI) and the respective specific primers enlisted in Table 4. The data were analyzed using STEPONE Software version 2.3 [Applied Biosystems (ABI)]. Fold changes were calculated using the formula $2^{-(Ct_{test}-Ct_{control})}$. β-actin or 18S rRNA was considered as housekeeping gene wherever applicable. Fold changes were calculated for at least three independent experiments and plotted as bar graphs with standard error of mean (SEM).

Antibodies

The antibodies used in this study were anti-FLAG (Sigma, F1804, Lot no. SLBK1346V), anti-NPM1 (in house-generated hybridoma clone 28M1), anti-tubulin (Calbiochem, Burlington, MA, USA, Cat No. CP06, Lot No. D00175772), anti-c-fos (Santacruz, Cat No. sc-52, Lot No. D2215), anti-c-jun (Abcam, Cambridge, UK, Cat No. ab7964, kindly gifted by Dr. Sagar Sengupta, National Institute of Immunology, India), anti-p53 (Calbiochem, Cat No. OP43, Lot No. 2635180), anti-GAPDH (in-house-generated polyclonal antibody), Goat Anti-Rabbit IgG H&L (HRP) (Abcam, Cat No. ab97051, Lot No. GR288027-9), Goat Anti-Mouse IgG H&L (HRP) (Abcam, Cat No. ab97023, Lot No. GR298142-12), F(ab')2-Goat anti-Rabbit IgG (H + L) Cross-Adsorbed Secondary Antibody, Alexa Fluor 488 (Life Technologies, Cat No. A11070, Lot No. 1618692), Goat anti-Mouse IgG (H + L) Highly Cross-Adsorbed Secondary Antibody, Alexa Fluor 633 (Life Technologies, Cat No. A21052, Lot No. 1712097) and F(ab')2-Goat anti-Mouse IgG (H + L) Cross-Adsorbed Secondary Antibody, Alexa Fluor 488 (Life Technologies, Cat No. A11017, Lot No. 1387827).

Chromatin immunoprecipitation

H1299 cells were maintained in RPMI-1640 supplemented with 10% FBS up to 80% confluency. ChIP experiments were performed as described previously [59]. Briefly, 10–15 million cells seeded in 100 mm dishes were cross-linked using 1% formaldehyde, followed by cell lysis in SDS lysis buffer

[1% SDS, 10 mM ethylenediaminetetraacetic acid (EDTA), 50 mM Tris–HCl, pH 8] and subjected to sonication using a Diagenode Bioruptor (Leige, Belgium) to produce DNA fragments of 100–300 bp in length using cold ChIP-dilution buffer (0.01% SDS, 1.1% Triton X-100, 1.2 mM EDTA, 16.7 mM Tris-HCl, pH 8, 167 mM NaCl). The lysates were pre-cleared prior to immunoprecipitation with pre-blocked Protein G-Sepharose (Amersham Biosciences, Buckinghamshire, UK) for 1 h. The pull-downs for ChIP assay was performed with anti-FLAG antibody or anti-c-fos antibody and pre-blocked Protein G-Sepharose beads which were incubated overnight. Beads were washed successively with low salt buffer (0.1% SDS, 1% Triton X-100, 2 mM EDTA, 20 mM Tris–HCl, pH 8, and 150 mM NaCl), high salt buffer (0.1% SDS, 1% Triton X-100, 2 mM EDTA, 20 mM Tris–HCl, pH 8, and 500 mM NaCl), LiCl buffer (250 mM LiCl, 1% NP40, 1% NaDOC, 1 mM EDTA, and 10 mM Tris–HCl, pH 8), and TE (10 mM Tris–HCl, pH 8, and 1 mM EDTA). Elution buffer (0.2% SDS and 100 mM $NaHCO_3$) was added to the washed beads, and the bead solution was incubated at room temperature (RT) for 30 minutes. The DNA-protein complexes were then reverse cross-linked by adding 200 mM NaCl, 20 μg Proteinase K (Sigma) and incubating at 65 °C for 4 h. Subsequently, 20 μg of RNaseA (Sigma) were added and was further incubated for 15 minutes at 37 °C. The immunoprecipitated DNA was extracted using phenol-chloroform, ethanol precipitated and used for real-time PCR analysis. The region-specific primer sets used for the real-time ChIP-qPCR analysis have been mentioned in Table 4.

Immunoprecipitation

H1299 cells seeded in 100 mm dishes were co-transfected with FLAG-c-fos and pCMV-R175H p53 constructs for 24 h followed by lysis in FLAG lysis buffer (50 mM Tris-HCl, pH 7.4, 150 mM NaCl, 1 mM EDTA, 1% Triton X-100, 10% glycerol and protease inhibitors). Immunoprecipitation was performed using M2 agarose beads (Sigma) using the manufacturer's protocol. The immunoprecipitated complex was eluted using 3X FLAG-peptide (Sigma) or 1X sample loading buffer followed by heating at 95 °C for 10 minutes. The eluted complex was electrophoresed on an SDS/PAGE gel and western blotting was performed with anti-c-fos and anti-p53 antibodies. Immunoprecipitation assays from AU565 cells were performed by lysing 10 million cells in RIPA buffer followed by incubation with 5 μg c-fos antibody or rabbit IgG and 25 μL of Dynabeads Protein G (Invitrogen) overnight. Beads were washed thrice with RIPA buffer and eluted using 1X sample loading buffer.

Immunohistochemistry and ethics statement

Oral tumor samples were collected from patients at Sri Devaraj Urs Academy of Higher Education and Research (SDUAHER), Kolar, Karnataka and the Bangalore Institute of Oncology (BIO), Bangalore, Karnataka. Ethical clearance was obtained from the Central Ethics Committee at SDUAHER, Kolar (Reference no. SDUAHER/KLR/R&D/79/2014-15), Ethical Review Board at BIO and Institutional Human Bioethics and Biosafety Review Committee at JNCASR (Reference no. JNC/IBSC/2013/07-1495), for this investigation. Written informed consent was obtained from all patients before collection of samples and sample collection procedures conformed to the Declaration of Helsinki standards. Immunohistochemistry was performed on tumor and adjacent normal tissues as described previously [60].

Immunofluorescence

For co-localization studies, H1299 cells were co-transfected with FLAG-R175H and FLAG-c-fos. After 24 h of transfection, cells were washed with 1X PBS and fixed by incubating in 4% paraformaldehyde in 1X PBS for 20 minutes at RT. Fixed cells were washed with wash buffer I (1X PBS) thrice and permeabilized by incubation in permeabilization buffer (1% Triton-X-100 in 1X PBS) for 5 minutes at RT. Cells were subsequently blocked with 5% fetal bovine serum (FBS) in IX PBS for 45 minutes at 37 °C, followed by incubation with primary antibodies, anti-p53 and subsequently anti-c-fos for 1 h at RT with intermediate washing with wash buffer II (1% FBS, 0.1% Triton-X-100 in 1X PBS). This was similarly followed by incubation with secondary antibodies anti-rabbit Alexa Fluor 488 and subsequently, anti-mouse Alexa Fluor 633. Immunostained cells were then incubated in 1 $\mu g \cdot mL^{-1}$ of Hoechst 33258 (Sigma) for 5 minutes at RT, washed thrice in 1X PBS and mounted on glass slides using 70% glycerol.

For characterization of doxycycline inducible expression of FLAG tagged R175H p53 in H1299 cells, cells were treated with or without doxycycline (Sigma, 1 $\mu g \cdot mL^{-1}$) for at least 24 h, followed by immunostaining using primary antibody anti-FLAG and secondary antibody anti-mouse Alexa Fluor 488 as per procedure mentioned above.

Imaging was performed in Carl Zeiss LSM 510 Meta Confocal Microscope at the JNCASR Imaging Facility, Bangalore, India.

Statistical analyses

Data are represented as mean and standard error of mean (Mean + SEM). All statistical analyses were performed using GRAPHPAD PRISM 7.0 software (GraphPad Prism Software Inc., San Diego, CA, USA). Comparison between two means were assessed by unpaired two-tailed Student's *t* test, and that between three or more groups were evaluated using one-way analysis of variance (ANOVA) followed by Tukey's post hoc test. A *P*-value of <0.05 was considered statistically significant. Figures were generated using ADOBE ILLUSTRATOR software (San Jose, CA, USA).

Acknowledgments

This work was supported by Jawaharlal Nehru Center for Advanced Scientific Research (JNCASR), Sir JC Bose Fellowship, Department of Science and Technology (DST), India (Grant No. SR/S2/JCB-28/2010), the Department of Biotechnology (DBT), India (Programme Support on 'Chromatin and Disease', Grant No. BT/01/CEIB/10/III/01 and Virtual National Oral Cancer Institute, Grant No. BT/PR17576/MED/30/1690/2016). PS and SD1 are supported by Council of Scientific and Industrial Research (CSIR) and University Grants Commission (UGC), India, respectively. TKK is a Sir J. C. Bose Fellow. We acknowledge Prof. Bert Vogelstein (Johns Hopkins University, Baltimore, MD) and Dr. Dirk Gründemann (University of Cologne, Germany) for the pCMV-wtp53 and pEBTetD SLC22A1 constructs, respectively and Dr. Sagar Sengupta (National Institute of Immunology, India) for the c-jun mammalian expression construct and antibody. We acknowledge Prof. Susanne M. Gollin (University of Pittsburgh) and Dr. Gautam Sethi (National University of Singapore) for providing us with the UPCI:SCC-29B and UM-SCC-1 cell lines, respectively. We also acknowledge the Confocal Imaging Facility at JNCASR, Bangalore, India.

Conflicts of interest

The authors declare that they have no conflicts of interest with the contents of this article.

Author contributions

PS designed the study, performed experiments, analyzed and interpreted the data and wrote the manuscript. SD1 performed experiments and analyzed the data. DS performed the luciferase assays and analyzed the data. SD2 generated the NPM1 promoter constructs. MK performed and analyzed the IHC data. SK made the p53 expression constructs. PS, SD1, DS, SD2, and TKK edited the manuscript. AM and GSK, being clinicians, provided patient samples and contributed to patient sample-derived data analysis. TKK conceived and coordinated the study and wrote the manuscript. All authors reviewed the results and approved the final version of the manuscript.

References

1 Grisendi S, Mecucci C, Falini B & Pandolfi PP (2006) Nucleophosmin and cancer. *Nat Rev Cancer* **6**, 493–505.
2 Tanaka M, Sasaki H, Kino I, Sugimura T & Terada M (1992) Genes preferentially expressed in embryo stomach are predominantly expressed in gastric cancer. *Cancer Res* **52**, 3372–3377.
3 Nozawa Y, Van Belzen N, Van der Made AC, Dinjens WN & Bosman FT (1996) Expression of nucleophosmin/B23 in normal and neoplastic colorectal mucosa. *J Pathol* **178**, 48–52.
4 Skaar TC, Prasad SC, Sharareh S, Lippman ME, Brünner N & Clarke R (1998) Two-dimensional gel electrophoresis analyses identify nucleophosmin as an estrogen regulated protein associated with acquired estrogen-independence in human breast cancer cells. *J Steroid Biochem Mol Biol* **67**, 391–402.
5 Shields LB, Gercel-Taylor C, Yashar CM, Wan TC, Katsanis WA, Spinnato JA & Taylor DD (1997) Induction of immune responses to ovarian tumor antigens by multiparity. *J Soc Gynecol Investig* **4**, 298–304.
6 Tsui KH, Cheng AJ, Chang P, Pan TL & Yung BY (2004) Association of nucleophosmin/B23 mRNA expression with clinical outcome in patients with bladder carcinoma. *Urology* **64**, 839–844.
7 Shandilya J, Swaminathan V, Gadad SS, Choudhari R, Kodaganur GS & Kundu TK (2009) Acetylated NPM1 localizes in the nucleoplasm and regulates transcriptional activation of genes implicated in oral cancer manifestation. *Mol Cell Biol* **29**, 5115–5127.
8 Pianta A, Puppin C, Franzoni A, Fabbro D, Di Loreto C, Bulotta S, Deganuto M, Paron I, Tell G, Puxeddu E *et al.* (2010) Nucleophosmin is overexpressed in thyroid tumors. *Biochem Biophys Res Commun* **397**, 499–504.
9 Gimenez M, Souza VC, Izumi C, Barbieri MR, Chammas R, Oba-Shinjo SM, Uno M, Marie SK & Rosa JC (2010) Proteomic analysis of low- to high-grade astrocytomas reveals an alteration of the expression level of raf kinase inhibitor protein and nucleophosmin. *Proteomics* **10**, 2812–2821.
10 Yun JP, Miao J, Chen GG, Tian QH, Zhang CQ, Xiang J, Fu J & Lai PB (2007) Increased expression of nucleophosmin/B23 in hepatocellular carcinoma and correlation with clinicopathological parameters. *Br J Cancer* **96**, 477–484.
11 Léotoing L, Meunier L, Manin M, Mauduit C, Decaussin M, Verrijdt G, Claessens F, Benahmed M, Veyssière G, Morel L *et al.* (2007) Influence of nucleophosmin|[sol]|B23 on DNA binding and transcriptional activity of the androgen receptor in prostate cancer cell. *Oncogene* **27**, 2858–2867.
12 Subong EN, Shue MJ, Epstein JI, Briggman JV, Chan PK & Partin AW (1999) Monoclonal antibody to prostate cancer nuclear matrix protein (PRO:4-216) recognizes nucleophosmin/B23. *Prostate* **39**, 298–304.
13 Weinhold N, Moreaux J, Raab MS, Hose D, Hielscher T, Benner A, Meissner T, Ehrbrecht E, Brough M, Jauch A *et al.* (2010) NPM1 is overexpressed in hyperdiploid multiple myeloma due to a gain of

chromosome 5 but is not delocalized to the cytoplasm. *Genes Chromosom Cancer* **49**, 333–341.
14 Sun Z, Yue L, Shen Z, Li Y, Sui A, Li T, Tang Q, Yao R & Sun Y (2017) Downregulation of NPM expression by Her-2 reduces resistance of gastric cancer to oxaliplatin. *Oncol Lett* **13**, 2377–2384.
15 Zeller KI, Haggerty TJ, Barrett JF, Guo Q, Wonsey DR & Dang CV (2001) Characterization of nucleophosmin (B23) as a Myc target by scanning chromatin immunoprecipitation. *J Biol Chem* **276**, 48285–48291.
16 Kondo T, Minamino N, Nagamura-Inoue T, Matsumoto M, Taniguchi T & Tanaka N (1997) Identification and characterization of nucleophosmin/B23/numatrin which binds the anti-oncogenic transcription factor IRF-1 and manifests oncogenic activity. *Oncogene* **15**, 1275–1281.
17 Ye K (2005) Nucleophosmin/B23, a multifunctional protein that can regulate apoptosis. *Cancer Biol Ther* **4**, 918–923.
18 Colombo E, Marine JC, Danovi D, Falini B & Pelicci PG (2002) Nucleophosmin regulates the stability and transcriptional activity of p53. *Nat Cell Biol* **4**, 529–533.
19 Feuerstein N & Mond JJ (1987) "Numatrin", a nuclear matrix protein associated with induction of proliferation in B lymphocytes. *J Biol Chem* **262**, 11389–11397.
20 Feuerstein N, Spiegel S & Mond JJ (1988) The nuclear matrix protein, numatrin (B23), is associated with growth factor-induced mitogenesis in Swiss 3T3 fibroblasts and with T lymphocyte proliferation stimulated by lectins and anti-T cell antigen receptor antibody. *J Cell Biol* **107**, 1629–1642.
21 Feuerstein N, Chan PK & Mond JJ (1988) Identification of numatrin, the nuclear matrix protein associated with induction of mitogenesis, as the nucleolar protein B23. Implication for the role of the nucleolus in early transduction of mitogenic signals. *J Biol Chem* **263**, 10608–10612.
22 Wu MH & Yung BY (2002) UV stimulation of nucleophosmin/B23 expression is an immediate-early gene response induced by damaged DNA. *J Biol Chem* **277**, 48234–48240.
23 Li J, Zhang X, Sejas DP, Bagby GC & Pang Q (2004) Hypoxia-induced nucleophosmin protects cell death through inhibition of p53. *J Biol Chem* **279**, 41275–41279.
24 Chan PK, Chan FY, Morris SW & Xie Z (1997) Isolation and characterization of the human nucleophosmin/B23 (NPM) gene: identification of the YY1 binding site at the 5′ enhancer region. *Nucleic Acids Res* **25**, 1225–1232.
25 Mai RT, Yeh TS, Kao CF, Sun SK, Huang HH & Wu Lee YH (2006) Hepatitis C virus core protein recruits nucleolar phosphoprotein B23 and coactivator p300 to relieve the repression effect of transcriptional factor YY1 on B23 gene expression. *Oncogene* **25**, 448–462.
26 Yeh CW, Huang SS, Lee RP & Yung BY (2006) Ras-dependent recruitment of c-Myc for transcriptional activation of nucleophosmin/B23 in highly malignant U1 bladder cancer cells. *Mol Pharmacol* **70**, 1443–1453.
27 Yung BY (2004) c-Myc-mediated expression of nucleophosmin/B23 decreases during retinoic acid-induced differentiation of human leukemia HL-60 cells. *FEBS Lett* **578**, 211–216.
28 Ren Z, Aerts JL, Pen JJ, Heirman C, Breckpot K & De Greve J (2015) Phosphorylated STAT3 physically interacts with NPM and transcriptionally enhances its expression in cancer. *Oncogene* **34**, 1650–1657.
29 Boudra R, Lagrafeuille R, Lours-Calet C, de Joussineau C, Loubeau-Legros G, Chaveroux C, Saru JP, Baron S, Morel L & Beaudoin C (2016) mTOR transcriptionally and post-transcriptionally regulates Npm1 gene expression to contribute to enhanced proliferation in cells with Pten inactivation. *Cell Cycle* **15**, 1352–1362.
30 Venters BJ & Pugh BF (2013) Genomic organization of human transcription initiation complexes. *Nature* **502**, 53–58.
31 Wasserman WW & Sandelin A (2004) Applied bioinformatics for the identification of regulatory elements. *Nat Rev Genet* **5**, 276–287.
32 Chiu R, Boyle WJ, Meek J, Smeal T, Hunter T & Karin M (1988) The c-Fos protein interacts with c-Jun/AP-1 to stimulate transcription of AP-1 responsive genes. *Cell* **54**, 541–552.
33 Curran T, Van Beveren C & Verma IM (1985) Viral and cellular fos proteins are complexed with a 39,000-dalton cellular protein. *Mol Cell Biol* **5**, 167–172.
34 Halazonetis TD, Georgopoulos K, Greenberg ME & Leder P (1988) c-Jun dimerizes with itself and with c-Fos, forming complexes of different DNA binding affinities. *Cell* **55**, 917–924.
35 Herschman HR (1991) Primary response genes induced by growth factors and tumor promoters. *Annu Rev Biochem* **60**, 281–319.
36 Bland KI, Konstadoulakis MM, Vezeridis MP & Wanebo HJ (1995) Oncogene protein co-expression. Value of Ha-ras, c-myc, c-fos, and p53 as prognostic discriminants for breast carcinoma. *Ann Surg* **221**, 706–718; discussion 718-20.
37 Bamberger AM, Milde-Langosch K, Rossing E, Goemann C & Loning T (2001) Expression pattern of the AP-1 family in endometrial cancer: correlations with cell cycle regulators. *J Cancer Res Clin Oncol* **127**, 545–550.
38 Wakita K, Ohyanagi H, Yamamoto K, Tokuhisa T & Saitoh Y (1992) Overexpression of c-Ki-ras and c-fos in human pancreatic carcinomas. *Int J Pancreatol* **11**, 43–47.

39 Yuen MF, Wu PC, Lai VC, Lau JY & Lai CL (2001) Expression of c-Myc, c-Fos, and c-jun in hepatocellular carcinoma. *Cancer* **91**, 106–112.
40 Healy S, Khan P & Davie JR (2013) Immediate early response genes and cell transformation. *Pharmacol Ther* **137**, 64–77.
41 Karin M, Liu Z & Zandi E (1997) AP-1 function and regulation. *Curr Opin Cell Biol* **9**, 240–246.
42 Turatti E, da Costa Neves A, de Magalhaes MH & de Sousa SO (2005) Assessment of c-Jun, c-Fos and cyclin D1 in premalignant and malignant oral lesions. *J Oral Sci* **47**, 71–76.
43 Sachdev R, Mandal AK, Singh I & Agarwal AK (2008) Progressive rise of c fos expression from premalignant to malignant lesions of oral cavity. *Med Oral Patol Oral Cir Bucal* **13**, E683–E686.
44 Neuberg M, Schuermann M, Hunter JB & Müller R (1989) Two functionally different regions in Fos are required for the sequence-specific DNA interaction of the Fos/Jun protein complex. *Nature* **338**, 589–590.
45 Consortium, E. P (2012) An integrated encyclopedia of DNA elements in the human genome. *Nature* **489**, 57–74.
46 Peng Y, Chen L, Li C, Lu W & Chen J (2001) Inhibition of MDM2 by hsp90 contributes to mutant p53 stabilization. *J Biol Chem* **276**, 40583–40590.
47 Freed-Pastor WA & Prives C (2012) Mutant p53: one name, many proteins. *Genes Dev* **26**, 1268–1286.
48 Peltonen JK, Helppi HM, Paakko P, Turpeenniemi-Hujanen T & Vahakangas KH (2010) p53 in head and neck cancer: functional consequences and environmental implications of TP53 mutations. *Head Neck Oncol* **2**, 36.
49 Kurki S, Peltonen K, Latonen L, Kiviharju TM, Ojala PM, Meek D & Laiho M (2004) Nucleolar protein NPM interacts with HDM2 and protects tumor suppressor protein p53 from HDM2-mediated degradation. *Cancer Cell* **5**, 465–475.
50 Maiguel DA, Jones L, Chakravarty D, Yang C & Carrier F (2004) Nucleophosmin sets a threshold for p53 response to UV radiation. *Mol Cell Biol* **24**, 3703–3711.
51 Rubbi CP & Milner J (2003) Disruption of the nucleolus mediates stabilization of p53 in response to DNA damage and other stresses. *EMBO J* **22**, 6068–6077.
52 Brady SN, Yu Y, Maggi LB Jr & Weber JD (2004) ARF impedes NPM/B23 shuttling in an Mdm2-sensitive tumor suppressor pathway. *Mol Cell Biol* **24**, 9327–9338.
53 Li J, Zhang X, Sejas DP & Pang Q (2005) Negative regulation of p53 by nucleophosmin antagonizes stress-induced apoptosis in human normal and malignant hematopoietic cells. *Leuk Res* **29**, 1415–1423.
54 Soussi T & Wiman KG (2015) TP53: an oncogene in disguise. *Cell Death Differ* **22**, 1239–1249.
55 Di Agostino S, Strano S, Emiliozzi V, Zerbini V, Mottolese M, Sacchi A, Blandino G & Piaggio G (2006) Gain of function of mutant p53: the mutant p53/NF-Y protein complex reveals an aberrant transcriptional mechanism of cell cycle regulation. *Cancer Cell* **10**, 191–202.
56 Frazier MW, He X, Wang J, Gu Z, Cleveland JL & Zambetti GP (1998) Activation of c-myc gene expression by tumor-derived p53 mutants requires a discrete C-terminal domain. *Mol Cell Biol* **18**, 3735–3743.
57 Teufel DP, Freund SM, Bycroft M & Fersht AR (2007) Four domains of p300 each bind tightly to a sequence spanning both transactivation subdomains of p53. *Proc Natl Acad Sci USA* **104**, 7009–7014.
58 Kroumpouzos G, Eberle J, Garbe C & Orfanos CE (1994) P53 mutation and c-fos overexpression are associated with detection of the antigen VLA-2 in human melanoma cell lines. *Pigment Cell Res* **7**, 348–353.
59 Das S, Senapati P, Chen Z, Reddy MA, Ganguly R, Lanting L, Mandi V, Bansal A, Leung A, Zhang S *et al.* (2017) Regulation of angiotensin II actions by enhancers and super-enhancers in vascular smooth muscle cells. *Nat Commun* **8**, 1467.
60 Shandilya J, Senapati P, Dhanasekaran K, Bangalore SS, Kumar M, Kishore AH, Bhat A, Kodaganur GS & Kundu TK (2014) Phosphorylation of multifunctional nucleolar protein nucleophosmin (NPM1) by aurora kinase B is critical for mitotic progression. *FEBS Lett* **588**, 2198–2205.